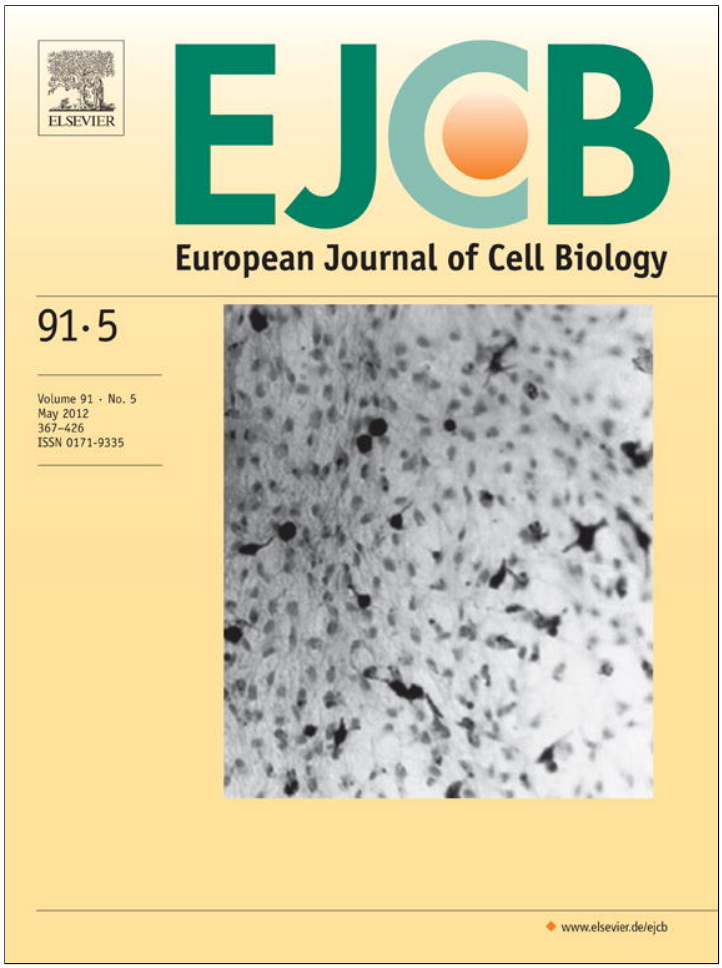

European Journal of Cell Biology 91 (2012) 375–390

Contents lists available at SciVerse ScienceDirect

European Journal of Cell Biology

journal homepage: www.elsevier.de/ejcb

Insights into Stem Cell Factor chemotactic guidance of neural crest cells revealed by a real-time directionality-based assay

Roberto A. Rovasio*, Laura Faas, Natalia L. Battiato

Centro de Biología Celular y Molecular, Facultad de Ciencias Exactas, Físicas y Naturales, Universidad Nacional de Córdoba, Av.Vélez Sarsfield 1611 (5016) Córdoba, Argentina

ARTICLE INFO

Article history:
Received 20 January 2011
Received in revised form
19 December 2011
Accepted 20 December 2011

Keywords:
Avian embryo
Cell migration
Chemotaxis
Melanocyte
Neural crest cells
Pigment cells
Skin
Stem Cell Factor

ABSTRACT

The extracellular environment through which neural crest cells (NCCs) translocate and differentiate plays a crucial role in the determination of cell migration and homing. In the trunk, NCC-derived melanocyte precursor cells (MPCs) take the dorsolateral pathway and colonize the skin, where they differentiate into pigment cells (PCs). Our hypothesis was that the skin, the MPCs' target tissue, may induce a directional response of NCCs toward diffusible factor(s). We show that the treatment of in vitro NCCs with skin extract (SE) or Stem Cell Factor (SCF) contributes to maintaining proliferative activity, accelerates melanocyte differentiation, and guides a subpopulation of NCCs by chemotaxis toward the gradient source of these factors, suggesting that they may represent the MPCs' subpopulation. Current data on stimulated directional persistence of NCCs supports the participation of diffusible molecules in the target colonization mechanism, guiding MPCs to migrate and invade the skin. Our results show similar effects of SE and SCF on NCC growth, proliferation and pigment cell differentiation. Also, the use of a proven real-time directionality-based objective assay shows the directional migration of NCCs toward SE and SCF, indicating that the epidermal SCF molecule may be involved in the chemotactic guidance mechanism of in vivo NCCs. Although SCF is the strongest candidate to account for these phenomena, the nature of other factor(s) affecting NCC-oriented migration remains to be investigated. This data amplifies the functional scope of trophic factors by involving them in new cell behaviors such as molecular guidance in the colonization mechanism of embryonic cells.

Introduction

In recent years, growing knowledge about cell communication at a distance has enabled the re-discovery of chemotactic phenomena, conceived as directional cell migration induced by a concentration gradient of soluble factors segregated by "target" fields. This molecular mechanism of cell orientation is well known in various biological systems such as flagellated bacteria (Chen et al., 2003), amoebas (van Haastert et al., 2007), leukocytes (Gómez-Moutón et al., 2004), neurons (Ng et al., 2005; Paratcha et al., 2006), and axonal growth cones (Charron and Tessier-Lavigne, 2005; Mortimer et al., 2008; von Philipsborn and Bastmeyer, 2007). In our laboratory, we made one of the first descriptions of the chemotaxis of mammal sperm toward the ovular region (Fabro et al., 2002; Giojalas and Rovasio, 1998; Giojalas et al., 2004a,b; Marín et al., 1995; Oliveira et al., 1999; Rovasio et al., 1994; Sun et al., 2003), with progesterone signals being the strongest attractant responsible (Guidobaldi et al., 2008; Teves et al., 2006). On the other hand, it is surprising that the embryonic cells, paradigmatic of accurately moving cells, have practically not been dealt with yet from a "chemotactic point of view" except in a few well documented systems on mouse embryos (Belmadani et al., 2005; Kubota and Ito, 2000; Natarajan et al., 2002; Young et al., 2004) and avian ambryos (Kasemeier-Kulesa et al., 2010; Tosney, 2004).

It is known that neural crest cells (NCCs), after segregating from the closing neural tube as a multipotent cell population, migrate along defined pathways and colonize precise sites giving rise to a variety of cell types, such as neurons, glia, cartilage and pigment cells (PCs) (Le Douarin and Kalcheim, 1999). In the modulation of such complex behaviors, the balance between the signals of a "central program" and those coming from the near milieu is not yet clear (see reviews by Kulesa et al., 2010; Krispin et al., 2010; Lock et al., 2008). However, there is growing evidence that indicates that the efficient migration and distribution of NCCs depends on coordinated genetic and epigenetic factors, specially triggered by micro-environmental signals (Kee et al., 2007; Le Douarin et al., 2007; Lock et al., 2008; Kulesa et al., 2010; Matthews et al., 2008a,b; Rovasio et al., 1983; Sauka-Spengler and Bronner-Fraser, 2008; Teddy and Kulesa, 2004; Wehrle-Haller et al., 2001). However, these factors are not sufficient to fully explain the oriented migration of NCCs. Moreover, the haptotaxis and galvanotaxis mechanisms lack sufficient supporting evidence

* Corresponding author. Tel.: +54 351 433 2097; fax: +54 351 433 2097.
E-mail address: rrovasio@efn.uncor.edu (R.A. Rovasio).

0171-9335/$ – see front matter © 2012 Elsevier GmbH. All rights reserved.
doi:10.1016/j.ejcb.2011.12.007

(Le Douarin and Kalcheim, 1999), and the rejection of a chemotactic mechanism claimed by some authors is not endorsed by rigorous experimental trials (Carmona-Fontaine et al., 2008; Erickson, 1985; Matthews et al., 2008a,b).

In the trunk, NCCs migrate in a dorsoventral pathway between the neural tube and the cephalic half of the somitic mesoderm (Le Douarin and Dupin, 1993), and a second wave between the somites and ectoderm is taken by the subpopulation of melanocyte precursor cells (MPCs) homing to skin (Erickson and Goins, 1995). The PCs are one of the most extensively studied NCC derivatives, since the pigment itself constitutes a unique differentiation marker. Moreover, it is known that the relationships between MPCs and their developmental milieu, and their timing, play key roles in the definition of PC distribution (Faas and Rovasio, 1998; Fukuzawa et al., 1995; Thibodeau and Frost-Mason, 1992).

In the avian embryo, MPCs colonize the skin between day 3 and 3.5 of development (Richardson and Sieber-Blum, 1993), and massively invade from day 5 to 6, when they proliferate (6th–8th day) and then differentiate into PCs from day 9 of development (Teillet, 1971). In a previous report, we showed that the spatial distribution of MPCs varies according to both the axial level and the developmental stage of the embryo; furthermore, the observed general pattern of the centrifugal double wave of cell distribution may be attributed to a different timing of cell differentiation, closely related to their migratory behavior (Faas and Rovasio, 1998). Considering the intrinsic motion capacity of NCCs together with the precisely timed colonization in the epidermis by MPCs, in both avian and mammalian embryos, it was suggested that the mechanism involved could be through a chemoattractant activity of the skin, its target tissue (Le Douarin and Kalcheim, 1999; Tosney, 2004). Thus, as with some other developmental systems, such as angiogenesis (Czirok et al., 2008), lymphocyte transmigration and homing (Cinamon et al., 2001), or genital ridge colonization by primordial germ cells (Boldajipour and Raz, 2007), the skin's product(s) could be involved in the regulation of PC colonization and development. Although the molecular cues to account for the proposed directional mechanism are not known, one of the strongest candidates is Stem Cell Factor (SCF), considering its in vivo expression in the target region (epidermis) of the NCC-derived MPCs, as well as the expression of its C-Kit receptor on this cell population (Lahav et al., 1994; Lecoin et al., 1995; see also Tosney, 2004). These molecular facts display a spatiotemporal coherence with the NCC colonization of the skin as well as their involvement with the differentiation of the pigment phenotype (Kunisada et al., 1998).

In this context, the present work reports the first direct evidence about the influence of embryo skin diffusible factors and SCF on the growth, proliferation, melanocyte differentiation and chemotactically oriented migration of the NCC subpopulation. These findings support the idea that SCF may serve as a specific chemoattractant for in vivo guidance of NCCs as well as having its canonic growth factor activity, amplifying the functional scope of trophic factors by involving them in new activities as molecular guides for embryonic cells. Last, but not least, the results here reported on turning responses of NCCs, in particular extracellular gradients of SCF, were obtained using a computer-based real-time video system and a software based on strictly proven objective directional criteria (Fabro et al., 2002; Giojalas and Rovasio, 1998; Ming et al., 1997, 1999; Rovasio et al., 1994; Song et al., 1997, 1998; Zheng et al., 1994).

Materials and methods

Skin extract

Quail embryos (Coturnix coturnix japonica) at 6–6.5 days of development (stages 22–23 of Zacchei, 1961) were incubated in deionized MilliQ water (Millipore Corp., Billerica, MA, USA) at 37 °C for 20 min, and the dorsal skin was mechanically removed using fine tweezers. The skin obtained from 63 embryos was centrifuged for 2 min at 5600 × *g* to remove the excess water, resuspended in N2 basal medium (Bottenstein and Sato, 1979) (50% DMEM and 50% F12 media, plus 15 mM sodium bicarbonate, 15 mM HEPES buffer, 50 IU/ml G sodium penicillin and 50 μg/ml streptomycin sulfate) without serum and homogenized in an ice bath. The homogenate was centrifuged for 15 min at 170,000 × *g* to remove cell debris, and the supernatant obtained was sterilized by filtration (0.22 μm, Renner GMBH, Dannstadt, Germany), aliquoted and stored at −40 °C until use. The total protein concentration was determined on the skin extract (SE) by Bradford's method (Bradford, 1976) and was taken as reference for the dilutions utilized. SDS-PAGE and Western blot analyses were performed using standard protocols on SE following conventional electrophoresis on 15% SDS-polyacrylamide gels. After transfer to polyvinylidene difluoride membranes (Millipore Corp., Billerica, MA, USA), primary antibody against SCF (rabbit polyclonal ab9753; 1 μg/ml; Abcam Inc., Cambridge, MA, USA) was used. Rat brain tissue lysate (Cat.# 1463; 20 μg per lane; ProSci Inc., Poway, CA, USA) and SCF (S7901; 1 per lane; Sigma Chem. Co., St Louis, MO, USA) were running as positive controls, all according to the indicated manufacturer's instructions.

Cell culture

Primary cultures of NCCs were made from mesencephalic and trunk levels of chick embryos (Gallus gallus, Cobb line) incubated at 38 ± 1 °C in a humidified atmosphere up to stage 11–14 HH (Hamburger and Hamilton, 1951; Rovasio and Battiato, 2002; Jaurena et al., 2011). Briefly, after cutting and opening the ectoderm, mesencephalic NCCs were carefully obtained by microdissection from the mass of NCCs bilateral to the neural tube, transferred to coverslips precoated with fibronectin (Rovasio et al., 1983), and incubated in 35 mm Petri dishes (Sigma Chem. Co., St Louis, MO, USA) with 2 ml of N2 defined medium (N2 basal medium plus 5 μg/ml insulin, 100 μg/ml transferrin, 20 nM progesterone, 100 μM putrescine and 30 nM selenium in 100 ml of medium) (Bottenstein and Sato, 1979) supplemented with 10% fetal calf serum (FCS) (Sigma Chem. Co., St Louis, MO, USA) during 24 h at 37 ± 0.2 °C in 5% CO_2 in air. Trunk explants corresponding to the last five to seven somite pairs were cut away and incubated with 200 μg/ml of dispase (Calbiochem Corp., San Diego, CA, USA) in N2 defined medium without serum for 15 min at room temperature. The segments of neural tube were isolated, washed with N2 medium plus 10% FCS, transferred to coverslips and incubated as explained. After 24 h, the neural tube explant was removed from the trunk NCC cultures to discard the possible source of undesired diffusible molecules, then the cultures were treated with 100 μl SE (or N2 defined medium = control), changing 50% of the culture medium every day during the time indicated below and in the Results section. Equivalent cultures, after neural tube explant removal, were utilized in chemotactic experiments.

Applying the careful microdissection technique described above, the degree of purity of NCC cultures was constantly near 100%, without neural tube, ectoderm and/or mesoderm contaminants. If some culture contained tissue contaminants, they were detected by phase contrast microscopy and NC-1 immunolabeling (Rovasio et al., 1983; Rovasio and Battiato, 1996), and consequently discarded. To verify for equal numbers of cells in control and SE/SCF-treated conditions at the beginning of the experiments, an estimation of NCC population considered the total cell number per explant at the start of the corresponding treatments (see Table 1 and Fig. 2, insets). Assuming that, operatively and based on embryo age, the initial size of the explants could be considered constant, we calculated the cell number per explant as statistically

Table 1
Growth parameters of neural crest cell cultures treated with skin extract (SE) and Stem Cell Factor (SCF).

Days of culture	Cell number[a]			Percentage of mitosis[a]			Cell outgrowth area[a,b]		
	Control	SE	SCF (50 ng/ml)	Control	SE	SCF (50 ng/ml)	Control	SE	SCF (50 ng/ml)
2	1009.00 ± 395.00	–	–	0.43 ± 0.12 *n*: 3000	–	–	4.20 ± 1.0 *N*: 6	–	–
3	1056.05 ± 380.50	3300.10 ± 900.05[c]	3550.20 ± 759.00[c]	0.42 ± 0.10 *n*: 2800	0.70 ± 0.05[c] *n*: 3200	0.73 ± 0.02[c] *n*: 3310	3.25 ± 0.9 *N*: 5	6.11 ± 0.8[c] *N*: 5	5.99 ± 0.9[c] *N*: 6
4	1275.57 ± 400.83	6928.33 ± 1032.87[c]	7087.39 ± 994.70[c]	0.48 ± 0.11 *n*: 3500	0.98 ± 0.04[c,d] *n*: 2200	1.09 ± 0.02[c,d] *n*: 2500	5.39 ± 1.5 *N*: 5	10.49 ± 0.9[c,d] *N*: 8	11.35 ± 0.5[c,d] *N*: 8
5	1451.56 ± 489.71	9715.09 ± 1137.40[c]	9935.10 ± 1003.10[c]	0.45 ± 0.05 *n*: 3500	1.70 ± 0.09[c,d] *n*: 3500	1.73 ± 0.08[c,d] *n*: 3650	7.81 ± 1.2 *N*: 7	15.97 ± 1.0[c,d] *N*: 9	16.99 ± 0.9[c,d] *N*: 8
6	2303.71 ± 588.23	11737.46 ± 1476.73[c]	12007.50 ± 1161.25[c]	0.42 ± 0.09 *n*: 7500	2.00 ± 0.10[c,d] *n*: 6500	2.08 ± 0.10[c,d] *n*: 6800	9.04 ± 2.3 *N*: 7	25.51 ± 1.1[c,d] *N*: 6	25.70 ± 1.3[c,d] *N*: 7

Differences between SE and SCF groups of the same culture stage are not significant. *n*: number of cells. *N*: number of explants.
[a] Mean ± s.e.m. The initial values at pre-treatment stage (2 days of culture) of control and SE or SCF groups were equivalent.
[b] Expressed in mm^2 as NCCs area (neural tube explant removed).
[c] Significant difference versus control.
[d] Significant difference versus the previous culture day.

equivalent at the start of each experimental run (Jaurena et al., 2011).

Cell counting, DOPA staining and evaluation of pigment cells

The effect of SE/SCF treatment on NCC growth and proliferation was estimated by comparing the total number of NCCs, the percentage of mitosis and the area occupied by NCC outgrowth. Parallel experiments were made to evaluate proliferation by using BrdU incorporation and antibody development (Jaurena et al., 2011), and no significant differences were shown compared with the previous method.

To detect pigment cells, a histochemical reaction was performed following a modification of the procedure described by Perris (1987). Cultures were fixed in 4% formaldehyde in phosphate buffer saline (PBS) pH 7.0, for 5 min at 4 °C, washed extensively in PBS and incubated in PBS containing 1% L-DOPA (Sigma Chem. Co., St Louis, MO, USA) for 4 h at 37 °C in the dark. The solution was changed each hour to prevent DOPA autooxidation. Following incubation, cultures were washed twice in PBS, post-fixed in 10% formaldehyde in PBS pH 7.4, for 12–24 h at 4 °C, and mounted with glycerin. The number of pigment cells (PCs) was scored every day under phase contrast microscopy, and the total numbers of NCCs and DOPA-positive cells were scored at the beginning (Day 2) and the end of each experiment (Days 3, 4, 5 and 6 of culture). Pigment cell differentiation was evaluated as the percentage of pigmented cultures/total cultures, in SE-treated and control cultures. The percentage of pigmented cultures with different degrees of pigmentation was scored for each experimental condition and classified into the following categories: none (absence of PCs), low (1–10 PCs/culture), medium (11–50 PCs/culture), high (51–100 PCs/culture) and very high (>100 PCs/culture).

Chemotaxis detection system

A modified chemotaxis chamber (Zigmond, 1977) was constructed with a Plexiglass plate of 70 mm × 30 mm × 3 mm in which two 20 mm × 4 mm × 2 mm parallel wells were drilled (Fig. 1A, B, w1, w2) (each one perforated with two holes at opposite ends, 1 mm diameter), separated by a partition wall 1.0 mm in width (Fig. 1A, p). After placing three small drops (~10 μl each) of N2 defined medium equidistant on the partition wall and spreading a small amount of sterile mineral oil with a cotton-bud on the surface of the plate outside the perimeter of both wells, a coverslip carrying the cultured NCCs was carefully mounted upside down on the chamber (Fig. 1A and B). The peripheral mineral oil and the small drops previously placed in the middle of the partition wall enabled two parallel closed chambers to be formed. The location of the NCC culture at the level of the partition wall and equidistant from both wells was verified under a stereoscopic microscope (Fig. 1A and B, cells). In the conventional manner, the left-hand well was perfused through the lateral hole with N2 medium using a tuberculin syringe with a 25 G needle, paying attention not to overflow toward the opposite well. After the air was eliminated through the opposite hole, the fluid just filled the capillary space between the partition wall and the coverslip, and both holes were stopped with small drops of mineral oil. Then, the right-hand well was filled with the SE or SCF (S7901; Sigma Chem. Co., St Louis, MO, USA) solution at the concentration indicated (or N2 medium = control), and both holes were also stopped with drops of mineral oil. Other experiments were carried out by filling the right-hand well with SE or SCF samples pre-incubated with 2 μg/ml of neutralizing anti-SCF antibody (rabbit polyclonal ab9753; Abcam Inc., Cambridge, MA, USA), or with heat-inactivated SCF. Some other experiments were carried out in the presence of anti-SCF or anti-C-Kit (1.5 μg/ml; monoclonal ab25495; Abcam Inc., Cambridge, MA, USA) antibodies in both wells, all according to the indicated manufacturer's instructions. Additional experiments of isotype control (IgG2b) were performed by using the same concentration of a monoclonal antibody (anti-melanoma mouse monoclonal ab14203; Abcam Inc., Cambridge, AM, USA) under the same blocking protocol.

This construction enabled the formation of a stable two-dimensional concentration gradient of diffusible molecules over a distance of a few hundred micrometers between both compartments, which was verified with a modification of a fluorescent method (Zheng et al., 1994; Zigmond, 1977) (Fig. 1C and D). Briefly, after the chamber was assembled as explained, the profile of the concentration gradient was quantitatively monitored by loading the right-hand well of the chamber with fluorescent reagents of different molecular weights: fluorescein isothiocyanate (FITC) isomer I 10% on celite, or 1 mM 5-carboxyfluorescein in N2 defined medium, or FITC-labeled IgG (Sigma Chem. Co., St Louis, MO, USA), and fluorescent images were collected with a ×10 objective for 9 h at 30 min intervals, then at 24 h, using a Hamamatsu C2400-08 camera with silicon-intensifier target tube (Hamamatsu Photonics K.K., Tokyo, Japan) (Fig. 1C). Densitometric graphs of intensity profiles of the fluorescent gradient measured pixel by pixel, enabled us to verify that a stable gradient was quickly established by diffusion over

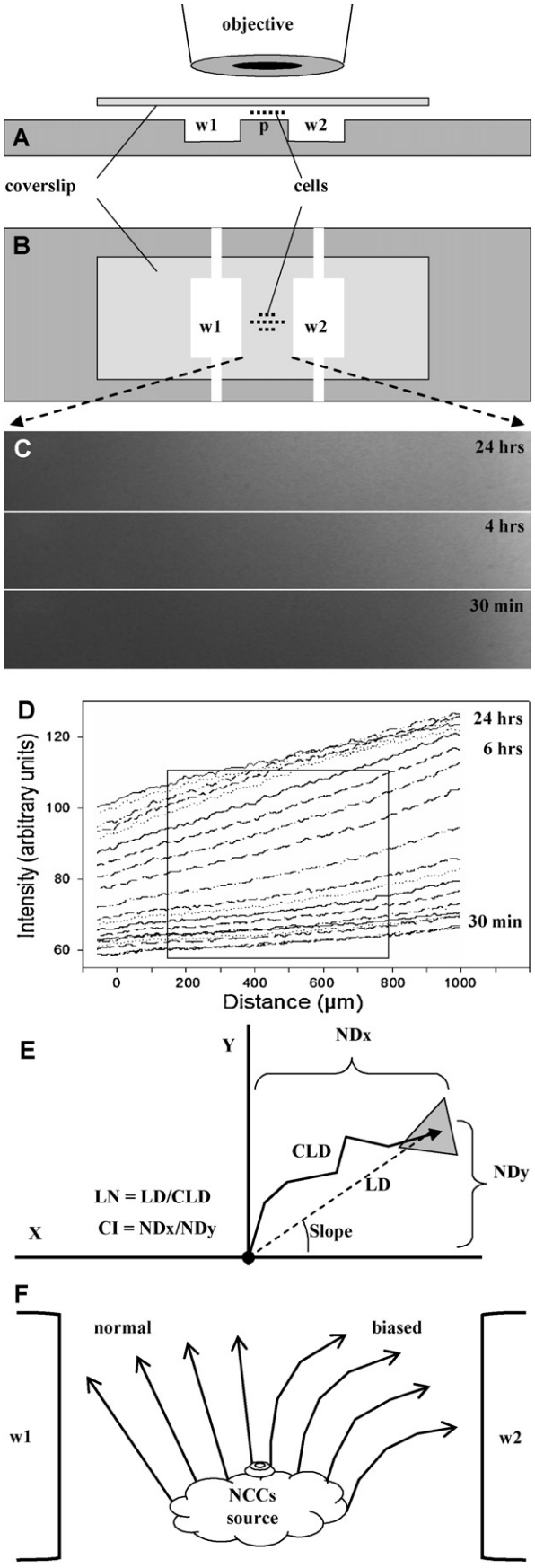

the entire width of the partition wall between both compartments (Fig. 1D). The steepness of the gradient between 200 and 800 μm from the source of the fluorescent molecule (across the microscopic field of about 600 μm × 500 μm as marked on Fig. 1D), was estimated as of 5–20° between 30 min and 9 h respectively (around 15 degrees at the end of 6 h of experimental time), values consistent with previous estimate data from equivalent systems (Lohof et al., 1992; Zheng et al., 1994).

After mountings, the chemotaxis chamber was placed on a 37 ± 0.1 °C thermostat-controlled plate of an Olympus BX-50 (Olympus Corp., Shinjuku-ku, Tokyo, Japan) microscope with a phase contrast optic, connected to a video-microscopy system consisting of a Sony SPT-M328CE video-camera (Sony Corp., Minato-ku, Tokyo, Japan), a DAGE-MTI HR1000 monitor (DAGE-MTI Technologies, Michigan, IN, USA), and a Sony SVT-S3050P video-recorder (Sony Corp.). Five minutes after the chamber sealing, the cells in the capillary space (~10 μm) between the coverslip and the middle of the partition wall were focused and video-recorded with a x10 objective (useful optic field ~600 μm × 500 μm). Recordings were carried out after focusing the cells of the migration front, and time-lapse video-microscopy was performed for 6 h at 1 frame every 1.5 s (Rovasio and Battiato, 1996, 2002). Then, cell images were captured with the VidCap tool by setting the video recorder in the playback mode (1 frame every 0.017 s, running continuously) and using the pause control at intervals of 30 min. Cell contours of each cell were outlined and transferred to a computer using commercial software (SigmaScanPro, SPSS, California, IL, USA) to analyze morphometric, dynamic and chemotactic parameters on the same samples of cells.

Some NCC cultures were fixed at the start and the end of the experimental time and stained for the actin cytoskeleton by applying the standard phalloidin-rhodamine reagent (Sigma Chem. Co., St Louis, MO, USA).

Morphometric and dynamic parameters

The following morphometric parameters were evaluated: (1) *Area;* (2) *Perimeter;* (3) *Compactness*, calculated as perimeter^2/area; (4) *Feret diameter*, calculated as the square root of 4 × area/π; (5) *Shape factor*, defined as (4π × area)/perimeter^2. The values of the three cell shape parameters were coherent, and we report here only the shape factor values. Because the shape factor of a circle is equal to the unit, the more an object lengthens, the more the shape factor tends to 0; and (6) *Binary center of mass* or "*centroid*", defined as the geometric center of a cell expressed as the average

Fig. 1. Chemotaxis detection system. (A) Transverse section, and (B) plane view of a Zigmond chamber under video microscopy equipment. A concentration gradient is formed between the coverslip and the partition wall (p) separating two wells (w1, w2). (C) Projection of the (fluorescent) gradient at the level of the partition wall at indicated intervals. (D) Densitometric graph of the fluorescent concentration gradient in function of the width of the microscopy field. The square included represents the limits of microscope field during recording (see details in the text). (E) XY coordinate system with the right side facing the source of the chemoattractant (or culture medium = control), related to some of the spatio-temporal cell parameters under study. A cell track is shown with the starting point at the origin (0,0) of the XY system and the final point in the area with highest probability of location of chemotactic responsive cells. CLD: curvilinear distance. LD: linear distance. LN: linearity. NDx: net distance parallel to the gradient. NDy: net distance perpendicular to the gradient. CI: chemotactic index. F: Schematic directional criteria for chemotactic behavior test, adapted from Ming et al. (1997, 1999), Song et al. (1997, 1998) and Zheng et al. (1994). NCCs migrating from a cephalic cumulus explant or an outgrowth of neural tube halo, located in the center of the partition wall (see details in the text), exhibited a centrifugal dispersion in the control condition or non responder cells (straight arrows on left-hand side), whereas under chemotactic signals from the right well (w2), the cell displacement—prevented from moving toward the explant—, show a biased trajectory pattern of movement (bent arrows on right-hand side).

of XY coordinates for every pixel in the cell perimeter, and is the initial calculation of every dynamic and chemotactic parameter of our user defined transformations (Fig. 1E).

As indicated in Fig. 1E, considering the X axis parallel to the gradient, the dynamic parameters determined were: (1) *Curvilinear distance* (CLD): represents the total distance traveled by the cell; (2) *Curvilinear velocity* (CLV): total distance traveled by the cell per unit time; (3) *Linear distance* (LD): the straight-line distance from the start to the final point of a cell trajectory; (4) *Linearity* (LN): nondimensional quotient between linear distance and curvilinear distance (LN = LD/CLD), is an estimator of the straightness capacity of a migratory cell, where the unit represents a rectilinear trajectory; (5) *Net distance in X* (NDx): the distance traveled between the initial and final points of the cell track projected on the X axis, the positive (right-hand) and negative (left-hand) distances being parallel to the chemotactic gradient; (6) *Net distance in Y* (NDy): the distance traveled between the initial and final points of the cell track projected on the *Y* axis, the positive (upper) and negative (lower) distances being perpendicular to the chemotactic gradient; and (7) *Steepness* (Slope): the declivity related to the gradient (*X* axis) between the initial and final points of the cell track (Fig. 1E).

In a first batch of experiments to approach the directional locomotion pattern(s) of NCCs, the mean-square-displacement and the diffusion coefficient were evaluated. Cell motility expressed as mean-square-displacement is the linear correlation between the square of the distance traveled and the experimental time, indicating that the motile cell behavior responds to the simple diffusion model based on random walk theory (Bray, 1992), the characteristics of which are determined by the theoretical parameters, root-mean-square speed and persistence time of direction. The root-mean-square speed is a mathematically derived determination of the speed of the cells which, unlike mean cell speed, is independent of the chosen time-interval between observations; and the persistence time of direction can be described as the average time between significant changes in the directional movement of a cell (Dunn, 1983; Gail and Boone, 1970). This evaluation of the global pattern of NCC locomotion supported the following stage of particular determination of chemotactic parameters.

Chemotactic parameters

In our chemotaxis detection system, it is essential to take into account several biological/experimental facts as well as the appropriate system geometry to evaluate the potential chemotactic behavior of the cells (Fig. 1F). Thus, in the embryo, NCCs migrate from the closing neural tube as a population of polarized substrate-attached cells, with temporary contacts among them (Teddy and Kulesa, 2004), and under the influence of the contact inhibition of locomotion (Carmona-Fontaine et al., 2008). The latter, in the context of a two-dimensional in vitro condition, produces a centrifugal migration that, after some hours of culture into a directionality-indifferent milieu, results in a smooth cell halo of outgrowth around the source explant. Consequently, in contrast to other free-swimming or isolated cells such as bacteria, spermatozoa or leukocytes, the undisturbed in vitro NCCs do not behave as isolated cells because (by reason of their explant origin) they do not show the same ability to move in any direction (Fig. 1F). Considering that the source of the NCCs, cephalic cell cumulus or trunk neural tube outgrowth, is positioned at the center of the partition wall, between the chamber wells, the cells that move without an oriented guide (control = no gradient) are physically prevented from going toward the explant but migrate in a centrifugal, fan-like dispersion (Fig. 1F, straight arrows on the left). However, under a two-dimensional gradient of chemotactic stimulus, the responsive cells show a clear bias of migratory pattern toward the attractant source (Fig. 1F, bent arrows on the right).

Two or more of the previously defined dynamic parameters were used to calculate the following chemotactic parameters, applying algorithms developed in our laboratory:

(1) *Percentage of cells migrating a net distance parallel to the gradient (X axis) greater than zero* (%NDx > 0): for cells exhibiting a random movement (control condition), the expected proportion of cells oriented to the right-hand or left-hand well should be ~50%, whereas it will be >50% for responsive cells migrating toward the attractant in a 180° angle (Oliveira et al., 1999).
(2) Percentage of cells with the quotient of the net distance parallel to the gradient (*X* axis) over the absolute value of the net distance perpendicular to the gradient (*Y* axis) greater than one (%NDx/|NDy|>1): for a cell population having equal possibilities to take any direction, the proportion of cells oriented toward any of the four quadrants of a two-dimensional microscopic field will be ~25%, whereas in a chemotactic field, the proportion of responsive cells oriented toward the quadrant of 90° angle facing the attractant gradient is expected to be higher than 25% (Fabro et al., 2002). Although this value is not reached in our experimental system because the cells are prevented from moving toward the explant but migrate fanwise, it is nevertheless a very good parameter for chemotaxis evaluation.
(3) *Mean of the net distance traveled by the cell parallel to the gradient (X axis)* ($\sum$NDx (+−)/total No. of cells): result of the algebraic sum of the net distances on the *X* axis of all cell tracks (+ and −) divided by the total number of cells. Alternatively, it is the positive net distances on the *X* axis minus the negative net distances, divided by the total number of cells. The value of this parameter is expected to be close to zero in a homogeneous, no-gradient, milieu (control condition) or with a population of non-responsive cells. In a chemotactic field with responsive cells migrating a longer distance toward the source of the attractant, the value of this parameter is expected to be higher than zero (Oliveira et al., 1999).
(4) *Chemotactic Index* (NDx (+−)/CLD): expresses the efficient distance traveled by a cell toward an attractant. It is calculated as the quotient of the net distances parallel to the gradient (*X* axis) of all the migrating cells divided by the total distance traveled (curvilinear distance). This parameter was the first "classical" measurement, after McCutcheon and colleagues, for quantifying the direction of migratory cells in relation to a chemotactic stimulus (McCutcheon et al., 1934); and this was also the beginning of the "quantitative era" employing time-lapse techniques (Noble and Levin, 1986). For cells responding to a chemotactic gradient, the value approaches a straight line (i.e. tends to 1), whereas for cells moving randomly the value tends to 0.
(5) *Turning angle in degrees* (Angle): expresses the directional bias of a moving cell responding to chemotactic gradient. This typically directional parameter is calculated as the arctangent transformation of the slope between the initial and final points of the cell tracks (Ming et al., 1997, 1999; Song et al., 1997, 1998; Zheng et al., 1994).
(6) *Turning angle as percentage of cells against, non-oriented or toward the attractant* (% negative, % non-oriented, % positive): the turning response is scored as the percentage of cells showing positive turning toward the attractant source (turning angle > 10°), no turning (|turning angle| = < 10°) or negative turning away from the attractant source (turning angle <−10°). The cut-off criterion for cell orientation was based on the value of 2× standard error of the mean (>95% confidence interval) of cell tracks in non-stimulated conditions (homogeneous control milieu). For NCCs evaluated in a Zigmond chamber with N2 defined medium in both wells, the turning response was −0.65 ± 4.09 (Mean ± s.e.m.). Thus, a track <−10° or >10° is

Table 2
Morphometric and dynamic parameters of neural crest cells in concentration gradients of Stem Cell Factor (SCF) and controls.

	Area (μm²)[a]	Perimeter (μm)[a]	SF[a]	CLD (μm)[a]	CLV (μm/h)[a]	LD (μm) [a]	LIN [a]
Control	2,292.06 ± 129.70	247.90 ± 17.03	0.48 ± 0.05	260.21 ± 11.97	43.37 ± 1.99	160.92 ± 9.30	0.63 ± 0.02
n: 79							
SCF 200 ng/ml	1,918.57 ± 139.82	204.49 ± 9.61	0.58 ± 0.05	216.77 ± 16.73	36.13 ± 2,79	148.09 ± 10.91	0.58 ± 0.04
n: 25							
	NS	NS	NS	NS	NS	NS	NS
SCF 100 ng/ml	2,003.14 ± 84.78	195.49 ± 16.98	0.66 ± 0.09	220.00 ± 19.15	36.66 ± 3.86	156.01 ± 11.19	0.62 ± 0.03
n: 39							
	NS	NS	NS	NS	NS	NS	NS
SCF 50 ng/ml	1,728.58 ± 80.56	290.59 ± 5.39	0.26 ± 0.05	215.90 ± 10.80	35.88 ± 2.80	130.49 ± 9.42	0.70 ± 0.02
n: 62							
	$p < 0.001$	$p < 0.04$	$p < 0.004$	$p < 0.009$	$p < 0.03$	$p < 0.03$	$p < 0.02$
SCF 25 ng/ml	1,604.33 ± 68.21	298.78 ± 9.81	0.23 ± 0.03	176.67 ± 7.99	29.44 ± 1.33	111.66 ± 6.32	0.73 ± 0.02
n: 91							
	$p < 0.001$	$p < 0.01$	$p < 0.001$	$p < 0.001$	$p < 0.001$	$p < 0.001$	$p < 0.001$
SCF 12.5 ng/ml	1,890.03 ± 131.38	232.80 ± 8.77	0.43 ± 0.02	233.00 ± 11.15	38.30 ± 1.86	152.88 ± 9.89	0.69 ± 0.03
n: 33							
	NS	NS	NS	NS	NS	NS	NS
SCF 25-Inac	2,164.91 ± 82.45	219.83 ± 15.98	0.56 ± 0.03	250.62 ± 11.26	41.44 ± 1.88	158.08 ± 8.20	0.66 ± 0.03
n: 50							
	NS	NS	NS	NS	NS	NS	NS

SF: Shape Factor. CLD: Curvilinear distance. CLV: Curvilinear velocity. LD: Linear Distance. LN: Linearity. Inac: Heat-inactivated. NS: Not significant. (n): Number of cells in each experimental condition. For the number of cell silhouettes evaluated, multiply by 13 in each experimental condition.

[a] Mean ± s.e.m.

considered left- or right-oriented respectively (Ming et al., 1997, 1999; Song et al., 1997, 1998; Zheng et al., 1994).

Statistical treatment

After estimation of the minimal sample size, no fewer than 50 cells and a mean of about 650 cell contours and centroids in each experimental condition repeated in triplicate were studied. The number of cells (and cell profiling of each cell) in each experimental condition is mentioned in the Results section. Means comparisons were made with Student's *t*-test and nonparametric Mann–Whitney tests. Analysis of proportions was performed with the *z*-test with Yates correction, or previous transformation to the corresponding arc-sine values, then one way ANOVA followed by Scheefee's method for comparing all contrasts (Montgomery, 1991), or the Tukey assay (Jaurena et al., 2011) performed using the SigmaStat (SPSS, California, IL, USA) software. Statistical significance was set at $p \leq 0.05$.

Results

Skin extract and chemotactic concentration of Stem Cell Factor induces proliferation and "motion-morphology" of in vitro neural crest cells

NCC cultures treated with pure skin extract (SE) showed a significant increase in the total number of cells per explant as well as a higher percentage of mitosis, compared to controls (Table 1). Proliferative data from BrdU incorporation revealed equivalent results (data not shown). These data are coherent with the cell outgrowth area occupied by NCCs, despite the reduction of individual cell area (see below, and Table 2), which is significantly larger in the SE-treated cultures, increasing also with increased incubation time, showing a notably extensive halo of outgrowing cells compared to control cultures (Table 1). Moreover, the number of NCCs, their proliferative rate and outgrowth area in cultures treated with SCF (50 ng/ml) were significantly higher than in the control condition and similar to values obtained with SE treatment (Table 1). On the other hand, growth parameters of NCC cultures treated with 1/10 or 1/50 dilutions of SE are not different from those of controls (data not shown).

In pure SE-treated cultures a uniform cell distribution was also seen with few cell-free spaces, as well as the typical stellate cell morphology, and scarce neurite-like processes (Fig. 2B, D, and F). In contrast, control cultures showed a significantly smaller halo of NCCs (Table 1), with a smaller cellular area and a high number of neurite-like processes connecting NCCs (Fig. 2A, C, and E).

Morphometric parameters were determined by applying real-time video-microscopy of NCCs under concentration gradients of SE, SCF and control conditions. Values representing the mean of 13 images per cell during 6 h of experimental time were obtained. When NCCs migrated in concentration gradients of 25 and 50 ng/ml of SCF at the source well, the cell area of moving cells showed a significantly decreased value with an increased perimeter (Table 2). Reduction of the shape factor was also seen at the same SCF concentrations (Table 2), indicating the lengthening experienced by migratory cells in a chemotactic milieu (see below), which corresponds with the typical distribution of cytoskeletal structure in SCF-exposed cells (see Fig. 7, insets). Similar values of these morphometric parameters were found in NCCs under gradients of SE at dilutions of 1/10 and 1/50 (data not shown).

Melanocyte differentiation increases after treatment of in vitro neural crest cells with skin extract or Stem Cell Factor

On NCC cultures of progressive incubation times after SE treatmet, the PCs showed their typical morphology with a variable number of cytoplasmic processes and a growing degree of pigmentation (Fig. 2B, D, and F), characteristics that were also seen on NCC cultures treated with SCF (Fig. 2F, inset). A higher magnification of these cultures shows up the spherical and elliptic morphology of melanosomes with variable pigmentation (Fig. 3A and B), suggesting different degrees of maturation (Provance et al., 1996), as well as proliferating melanocytes (Fig. 3B, inset).

In preliminary experiments, we observed a high proportion of pigment cells (PCs) on the 4th day of culture in both control and pure SE-treated cultures, showing a high variability in their values, probably due to the remarkable increase in the number of NCCs at that time of incubation (Table 1). Therefore, we estimated the melanocytic differentiation as the proportion of pigmented NCC cultures, which were classified in five degrees of pigmentation (see Material and Methods). Results summarized in Fig. 4 clearly show that, at the 3rd day of culture, 62% of controls versus 37% of

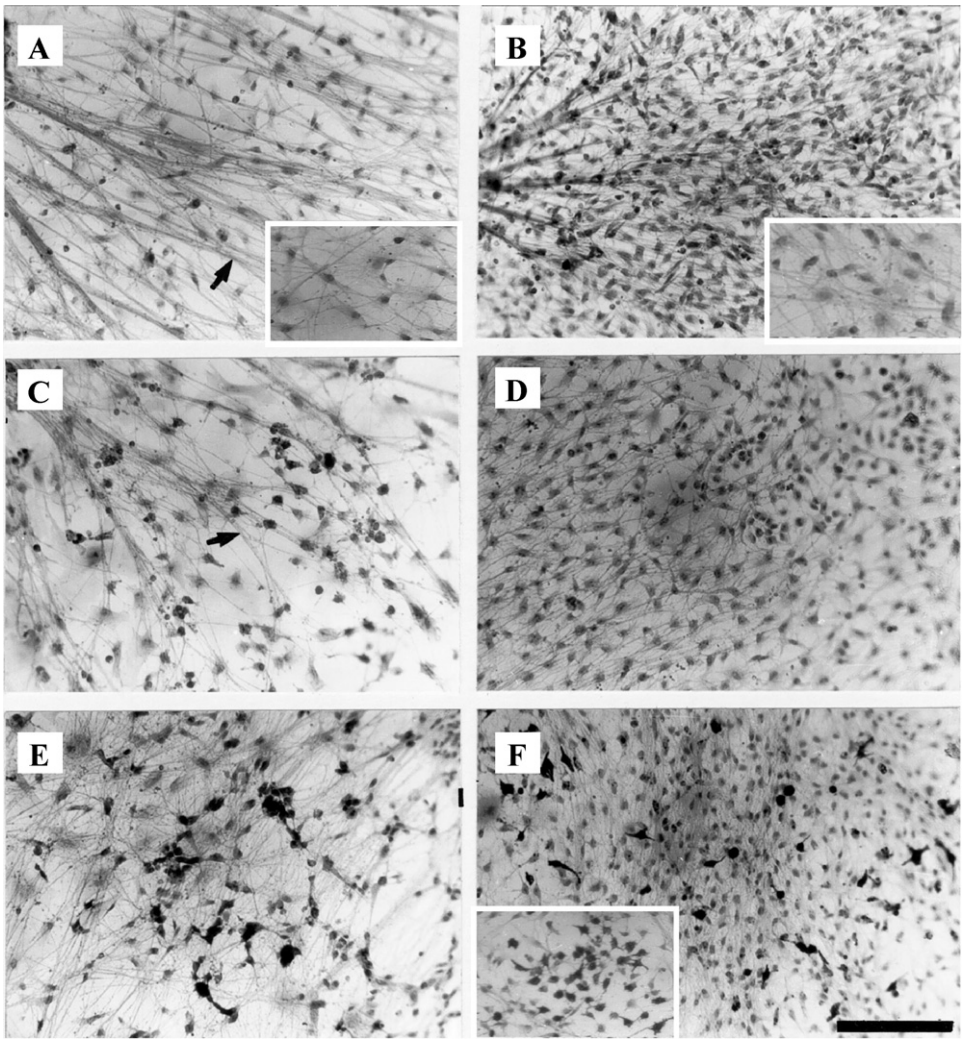

Fig. 2. NCC cultures of 4 (A, B); 5 (C, D) and 6 (E, F) days, controls (A, C, E) and pure SE-treated (B, D, F). Insets on (A) and (B) show NCC cultures at the start of the corresponding experiments. Inset on (F) shows a NCC culture after treatment with SCF. In all cases, the neural tube explant was removed. Note the enlarged cell density, the low development of neurite-like processes (arrows) and the increasing pigmentation in cultures treated with SE/SCF. Phase contrast optic. Bar: 160 μm 100×.

SE-treated cultures remained unpigmented. These percentages tended to decrease with culture time, reaching zero at day 4 of culture in SE-treated experiments, while in controls they reached zero at day 5. On the other hand, the cell proportion with a very high degree of pigmentation in control cultures increased with the course of time, from zero at the 3rd day of culture reaching 66% at day 6, while the SE-treated cultures showed a very high degree of pigmentation, increasing from 6% at the 3rd day of culture to 86% by day 6 (Fig. 4). The experiments carried out using culture treatments with 1/10 or 1/50 dilutions of SE did not show results significantly different from the controls.

Changes of dynamic parameters and chemotactic response are induced on in vitro neural crest cells by concentration gradients of skin extract or Stem Cell Factor

A preliminary goal of this study was to establish a reliable, directionality-based, objective method for the evaluation of chemotaxis, independently of chemokinesis and other dynamic phenomena. This is essential because, to assert chemotactic cell behavior, it is not sufficient to show anisotropic cell accumulation, as this could also be biased by effects of cell speed, pattern of movement, trapping phenomena or trophic effects (Eisenbach, 1999; Fabro et al., 2002). For this reason, we employed a real time video-microscopy approach and a directionality-based algorithm, using a chemotaxis chamber (Zigmond, 1977), thus avoiding interference from processes other than chemotaxis which might cause selective accumulation of cells (Fabro et al., 2002; Marín et al., 1995; Rovasio et al., 1994).

The dynamic behavior of NCCs exposed to concentration gradients of 1/10 or 1/50 dilution of SE in the source revealed an active and global cell response typical of directional migration. As a first and abridged characterization of the locomotion patterns of NCCs exposed to a gradient of 1/50 dilution of SE and control, the mean-square-displacement and the diffusion coefficient are shown in both conditions (Fig. 5). Our results on NCCs migrating in the Zigmond chamber indicate that the migratory pattern is diffusive in a 1/50 dilution of SE-treated cultures (Fig. 5), exhibiting a higher diffusion coefficient than the control (Fig. 5, inset). This result agrees with the increasing linearity of cells exposed to SE gradient. Thus, preliminary observations suggested that the distance traveled, velocity, linearity and chemotactic bias are coherently related and involved in a progressive and oriented motion of the cell toward factor(s) segregated by the skin.

Dynamic and chemotactic cell behavior data obtained with the same cluster of parameters applied in NCCs under chemotactic concentrations of SE and SCF were not significantly different and we will show henceforth only the detailed results corresponding to

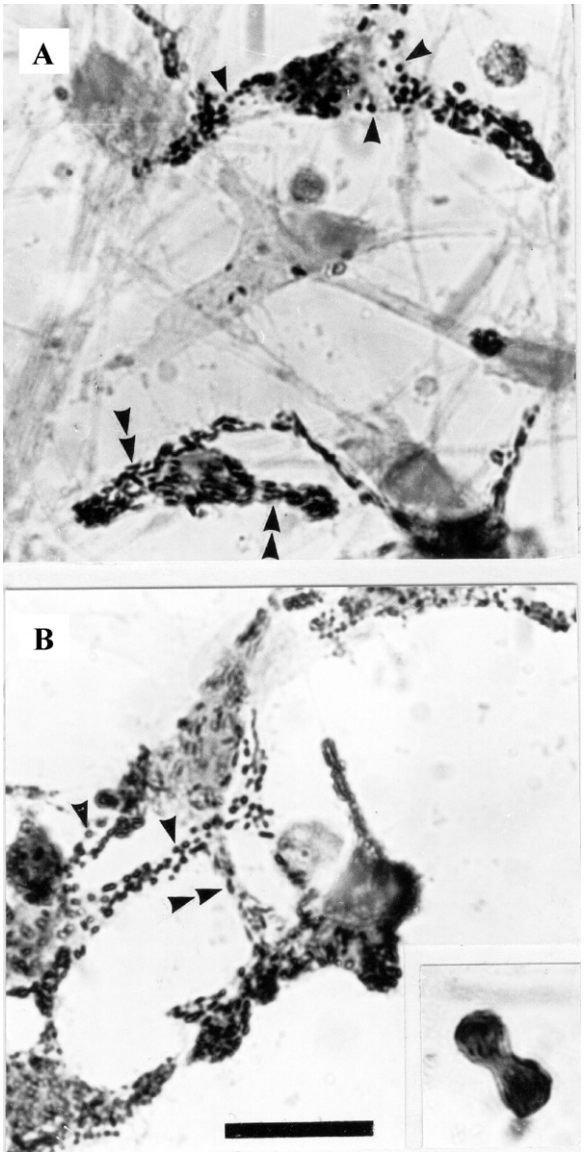

Fig. 3. NCCs of 5 (A) and 6 (B) day cultures treated with pure SE. Dopa staining. Note variations in the number and morphology of melanosomes from spherical (arrowhead) to elliptic (double arrowhead). Mitoses are also observed in the pigment cells (inset). Phase contrast optic. Bar: 20 μm. ×800. Similar aspect was seen after treatment with SCF (50 ng/ml).

the SCF-treated groups. The functional blocking experiments using anti-SCF or anti-C-Kit antibodies (see Materials and Methods section) also gave similar results to those using heat-inactivated SCF, so we show here only results of the latter condition. Functional blocking experiments to control monoclonal antibody isotype gave non-significantly different results from those using SCF alone (data not shown), showing the specificity of the functional blocking.

After exposure at concentration gradients of 25 or 50 ng/ml of SCF in the source (chemotactic concentrations, see below), the absolute distance and velocity, as well as the linear distance traveled by the NCCs, were significantly lower compared to higher or lower SCF concentrations or to controls (Table 2). Cell linearity, as a nondimensional parameter characterizing the capacity of the cell to maintain a straight trajectory, was higher at 25 and 50 ng/ml of SCF concentrations in the source (Table 2).

These results supported SCF as a strong candidate for the attraction of pre-melanocyte NCCs to the skin. Thus, cultures under concentration gradients of SCF showed significant chemotactic behavior of NCC subpopulations at concentrations of 25 or 50 ng/ml of SCF at the gradient source. This oriented behavior was expressed as the percentage of cells migrating a net distance parallel to the gradient greater than zero, that is more cells moving into an angle of 180° facing the SCF, while only about 50% of cells migrated to the control milieu (Table 3, first column; Fig. 6, black columns). Chemotaxis was also revealed under a more stringent test, expressed as cells that move in a much more oriented way into an angle of 90° facing the SCF (Table 3, second column; Fig. 6, grey columns). Lower and higher SCF concentrations did not induce chemotactic migration. Moreover, when SE or chemotactic concentrations of SCF (25 or 50 ng/ml) were pre-incubated with anti-SCF or assayed in the presence of anti-C-Kit antibodies, the values of oriented migration of NCCs fall to the control condition (Fig. 6). Since there were no significant differences between treatments with anti-SCF, anti-C-Kit antibodies or heat-inactivated SCF, the values of these conditions were subsequently shown as inactivated SCF (Figs. 7–11, 25-Inac). At the higher concentration of 200 ng/ml of SCF, the percentage of chemotactic NCCs was significantly lower than in controls (Table 3, first and second columns; Fig. 6).

Both 25 and 50 ng/ml of SCF in the gradient source also showed a chemo-attractant effect when the chemotactic parameter was expressed as the mean of the net distance traveled parallel to the SCF gradient, but the treatment with 200 ng/ml of SCF promoted a significant chemo-repulsive reaction (Table 3, third column; Fig. 7). As mentioned, NCCs experiencing chemotactic migration showed cell lengthening and a typical distribution of the actin cytoskeleton as compared to controls (Fig. 7, insets).

Considering that the chemotactic index expresses how biased a cell trajectory is, since it is expressed as the quotient between the net distance parallel to the gradient and the total distance traveled by the cell, it also confirms the chemo-attraction of NCCs exposed to gradients of 25 and 50 ng/ml SCF, as well as the chemo-repulsion after placing 200 ng/ml of SCF in the gradient source (Table 3, fourth column; Fig. 8). Once more, this parameter shows that NCC chemotactic behavior is prevented by anti-SCF or anti-C-Kit antibodies, or heat-inactivated SCF (Fig. 8, 25-Inac). Moreover, a clear expression of the C-Kit receptor was found on the majority of NCCs at the leading front, supporting the selective directional response of this cell population toward the SCF (Fig. 8, insets).

The turning angle of the chemotactic response is another important parameter of migratory cell behavior, much applied in studies of chemotactic axonal growth cone (Ming et al., 1997, 1999; Song et al., 1997, 1998; Zheng et al., 1994), and adapted to our system. They express the mean value in degrees of the slope between the initial and final points of the cell track. This parameter also showed the positive and negative chemotactic behavior of NCCs in SCF gradients at concentrations of 25–50 or 200 ng/ml respectively in the source (Table 3, right; Fig. 9). When the turning response of migratory NCCs was evaluated as the proportion of cell tracks that are non-oriented, or oriented toward or against the SCF source, it was clearly seen that, at a chemo-attractant concentration of 25 and 50 ng/ml SCF there was a higher percentage of cells oriented to gradient (Table 3, far right; Fig. 10), while the subpopulation of NCCs chemo-repelling at 200 ng/ml SCF in the source matched well with a low proportion of cells non-oriented or oriented toward the SCF.

The position of every cell at the end of each experiment also shows the biased location of NCCs toward the gradients of 25 and 50 ng/ml SCF when it is expressed as cumulative turning angles of cell tracks at the end of 6 h of experimental time (Fig. 11A, a,b), and the repulsive cell behavior (Fig. 11A, c), compared with the equidistant distribution plots of the control conditions (Fig. 11). Moreover, the chemotactic effect is clearly visualized after plotting the linear distance expressed as the straight line from the start to the final points of a cell trajectory after exposure to control (Fig. 11B) or to the SCF chemotactic gradient (Fig. 11C). As was previously stated,

Table 3
Chemotactic parameters of neural crest cells in concentration gradients of Stem Cell Factor (SCF) and controls.

	% of cells migrating to the attractant	% of cells migrating straight to the attractant	Distance traveled toward the attractant (μm) [a]	Chemotactic Index [a]	Turning responses in relation to the attractant					
					In degrees[a]			In % of cells[b]		
					<−10°	>−10° < 10°	>10°	Against	Non oriented	Toward
Control (*n*: 79)	49.1	5.06	1.07 ± 6.59	−0.002 ± 0.03	−31.29 ± 5.43 (*n*: 29) Mean: −0.65 ± 4.09	−0.24 ± 1.35 (*n*:.22)	30.76 ± 5.56 (*n*: 28)	36.71 *NS	27.85	35.44
SCF 200 ng/ml (*n*: 25)	24 $p < 0.05$	1.6 NS	−33.53 ± 12.35 $p < 0.02$	−0.16 ± 0.06 $p < 0.008$	−63.71 ± 10.52 (*n*:17) $p < 0.002$ Mean: −21.52 ± 15.96 $p < 0.007$	1.43 ± 3.26 (*n*:3) NS	108.18 ± 18.33 (*n*:5) $p < 0.002$	68 $p < 0.02$ *$p < 0.003$	12 NS	20 NS
SCF 100 ng/ml (*n*: 39)	48.72 NS NS	2.56 NS	0.86 ± 8.87 NS	0.01 ± 0.04 NS	−40.94 ± 8.71 (*n*: 10) NS Mean: −3.30 ± 4.66 NS	−0.52 ± 1.53 (*n*: 17) NS	24.14 ± 3.30 (*n*: 12) NS	25.64 NS	43.59 NS	30.77 NS *NS
SCF 50 ng/ml (*n*: 62)	72.58 $p < 0.008$	17.74 $p < 0.03$	39.95 ± 10.23 $p < 0.002$	0.18 ± 0.04 $p < 0.001$	−52.55 ± 12.69 (*n*: 11) NS Mean: 13.57 ± 5,27 $p < 0.003$	2.03 ± 1.34 (*n*: 15) NS	38.58 ± 3.38 (*n*: 36) $p < 0.02$	17.74 $p < 0.03$	24.19 NS	58.06 $p < 0.02$ *$p < 0.001$
SCF 25 ng/ml (*n*: 91)	72.53 $p < 0.003$	21.98 $p < 0.004$	34.10 ± 6.43 $p < 0.001$	0.18 ± 0.04 $p < 0.001$	−49.59 ± 9.44 (*n*: 17) $p < 0.04$ Mean: 29.07 ± 6.17 $p < 0.001$	1.09 ± 1.58 (*n*: 14) NS	58.90 ± 5.84 (*n*: 60) $p < 0.001$	18.68 $p < 0.02$	15.38 NS	65.93 $p < 0.001$ *$p < 0.001$
SCF 12.5 ng/ml (*n*: 33)	54.55 NS	6.06 NS	−0.25 ± 11.26 NS	0.008 ± 0.05 NS	−34.59 ± 5.19 (*n*: 11) NS Mean: −1.01 ± 5.35 NS	0.32 ± 1.93 (*n*: 10) NS	28.65 ± 5.45 (*n*: 12) NS	33.33 NS	30.3 NS	36.36 NS *NS
SCF 25-Inac (*n*: 50)	44 NS	8 NS	−3.62 ± 8.01 NS	−0.004 ± 0.04 NS	−29.32 ± 5.79 (*n*: 17) NS Mean: 2.73 ± 6.62 NS	−2.92 ± 1.36 (*n*: 15) NS	33.20 ± 5.21 (*n*: 18) NS	34 NS	30 NS	36 NS *NS

All statistical comparisons versus the control condition, except (*) against the opposite turning responses.

[a] Mean ± s.e.m.

[b] *z*-test with Yates correction. (*n*): number of cells per experimental group. Inac: heat-inactivated. NS: not significant.

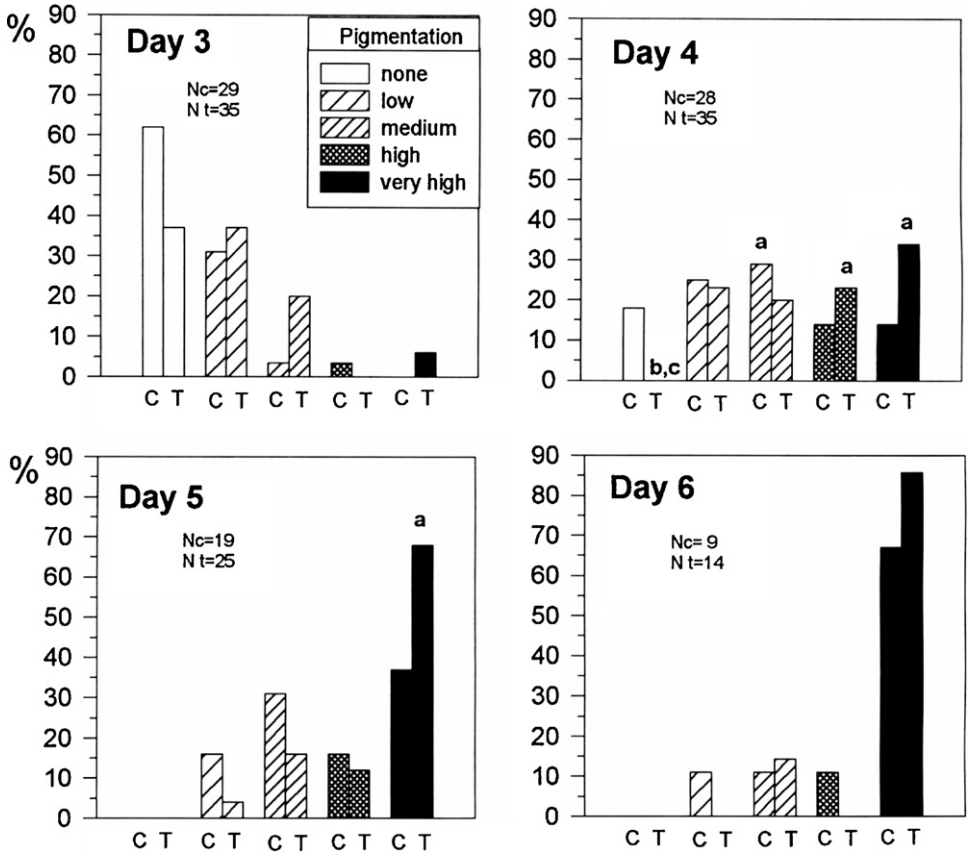

Fig. 4. Different degrees of NCC pigmentation expressed as percentage of pigmented cultures in SE-treated (T) and control (C) conditions, after 3, 4, 5 and 6 days of incubation. See criteria for classification in Materials and Methods. Proportion of pigmented cultures was transformed to arc-sine values to check for statistical differences. Significant difference with the previous culture day: (a) $p < 0.05$; (b) $p < 0.001$ and with control cultures: (c) $p < 0.05$. Nc: number of control explants. Nt: number of SE-treated explants.

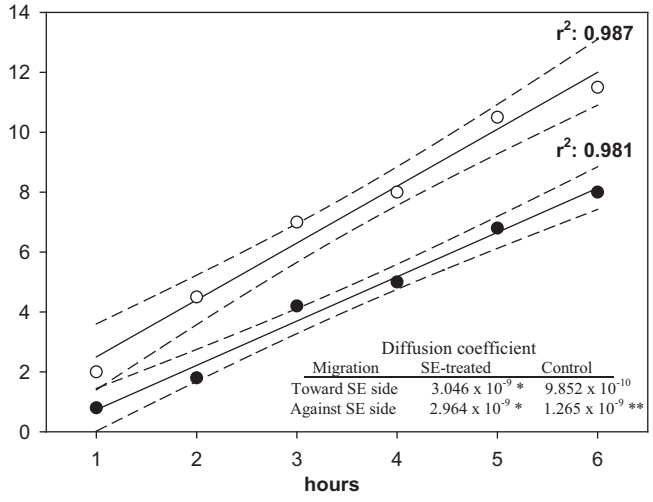

Fig. 5. Mean square displacement of NCCs exposed to SE-gradient (○) and control (●). r^2: linear regression coefficient ($p < 0.05$). Dashed lines: regression fitting with 95% confidence interval (- - -). Diffusion coefficient (cm^2/seg). On the *Y*-axis: 1×10^3 μm^2. Significant differences * versus control, ** versus opposite side.

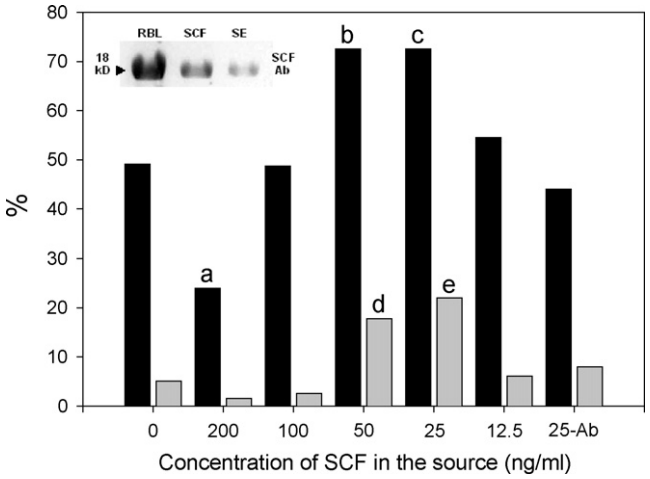

Fig. 6. Proportion of NCCs migrating up to gradients of SCF. Chemotaxis is expressed as the percentage of cells migrating to the SCF-gradient into a 180° angle (black columns), and into a 90° angle (grey columns) (see Materials and Methods for definitions). Proportion of migrating NCCs was transformed to arc-sine values to check for statistical differences. Western blot (inset) show immunolabeling of SCF in a sample of SE, using rat brain tissue lysate (20 μg per lane, RBL) and SCF (1 μg per lane) as positive controls (see Materials and methods for details). Columns marked 25Ab represent pre-treatment of 25 ng/ml SCF with anti-SCF antibody. Since no significant difference was seen among the pre-treatment with anti-SCF, or in the presence of anti-C-Kit antibody, or with heat-inactivate SCF, henceforth the values of these experimental conditions will be show as inactivate SCF (25-Inac). Significant differences versus control a: $p < 0.05$; b: $p < 0.008$; c: $p < 0.003$; d: $p < 0.03$; e: $p < 0.001$.

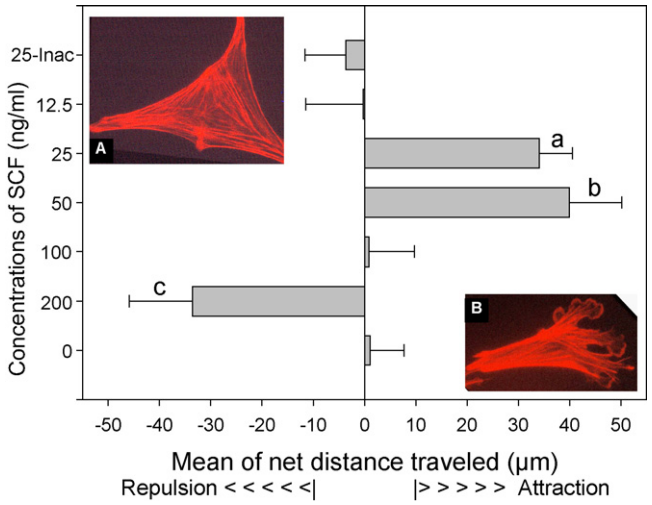

Fig. 7. Distance traveled by NCCs in gradients of SCF. Chemotaxis is expressed as the mean of the net distance traveled parallel to the gradient (*X* axis). Significant differences versus control: a: $p < 0.001$; b: $p < 0.002$; c: $p < 0.02$. Quiescent (A) and migrating (B) NCCs, actin cytoskeleton stained with phaloidin-rhodamine.

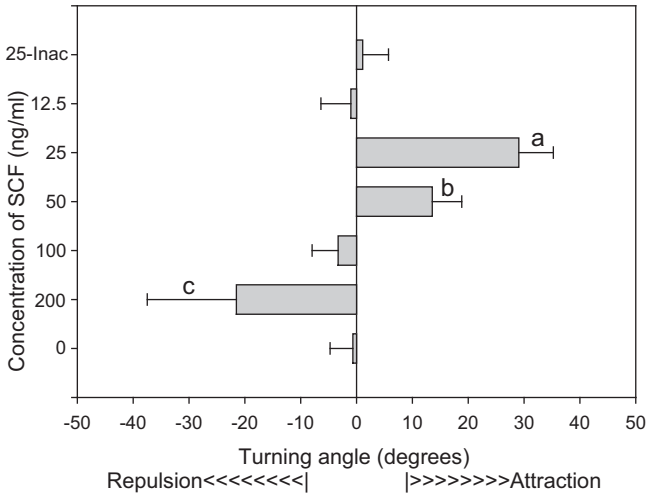

Fig. 9. Turning responses of migratory NCCs in gradients of different SCF concentration. Chemotaxis is expressed as the mean of the turning angle (in degrees) of cell tracks between the start and final points of migration. Significant differences versus control. a: $p < 0.001$; b: $p < 0.003$; c: $p < 0.007$.

chemotactic response was not observed when anti-SCF or anti-C-Kit antibodies were present in the system medium, and these values were not significantly different from those of the heat-inactivated SCF.

Discussion

One of the most intriguing and complex problems in developmental biology is the foundation of the cell's ability to distribute into particular fields of the body. Although in recent decades much biological knowledge has converged toward the molecular definition of migratory cell behavior, satisfactory explanations about the mechanism(s) for the precise orientation of the embryonic cells are as yet scarce. A plausible process involving the directional communication of the cell reverts to the old concept of chemotaxis, advanced for axon growth cones at the end of 19th century (Ramón y Cajal, 1892), as the capacity of the cell to recognize distant guide signals arising from a spatio-temporal concentration gradient, and consequently responding with an oriented displacement toward the specific soluble factor(s) segregated by "target" fields (Belmadani et al., 2005; Natarajan et al., 2002; Tosney, 2004; Wang et al., 2007). Over the past 15 years, this guidance mechanism was "re-discovered" by researchers making spectacular contributions on the pathfinding behavior of the axon growth cone (Charron and Tessier-Lavigne, 2005; Mortimer et al., 2008; von Philipsborn and Bastmeyer, 2007); now we wait hopefully for reports focusing on another accurately moving paradigm, the embryonic cells (see Kasemeier-Kulesa et al., 2010).

The neural crest cells (NCCs), a well-known example of this paradigm, form a multipotent cell population of the vertebrate embryo, undergoing wide dispersion along multiple pathways, and finally invading and colonizing with high precision particular sites

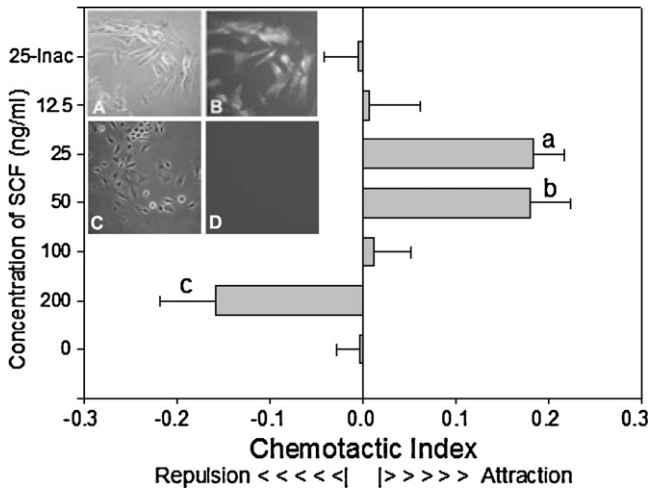

Fig. 8. Chemotactic index of NCCs in gradients of SCF. Chemotaxis is expressed as the quotient between the net distance parallel to the gradient (*X* axis) and the total distance traveled. Significant differences versus control condition. a: $p < 0.001$; b: $p < 0.001$; c: $p < 0.008$. Insets show immunolabeling of the C-Kit receptor at the leading front of NCC culture (A, B), and at the "rear" area of the explants (C, D). A, C: phase contrast. B, D: immunolabeling.

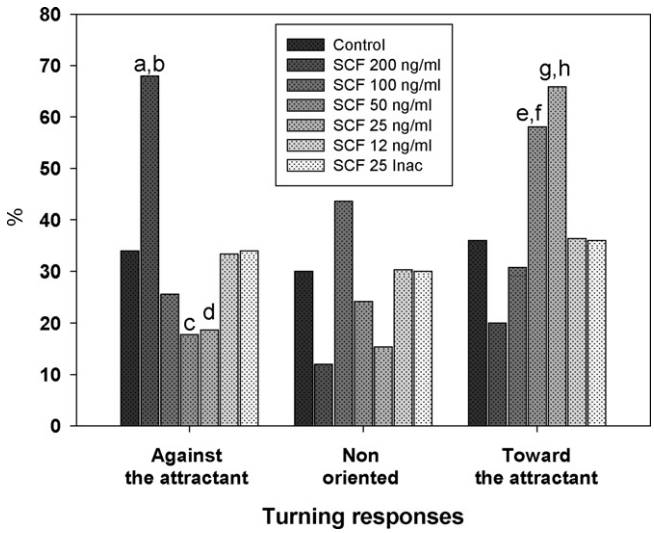

Fig. 10. Proportion of turning responses of NCCs in gradients of different SCF concentrations. Chemotaxis is expressed as percentages of cell tracks not oriented or turning toward or against the gradient. Proportion of turning NCCs was transformed to arc-sine values to check for statistical differences. Significant differences: a: $p < 0.02$ versus Control. b: $p < 0.003$ versus Toward the attractant. c: $p < 0.03$ versus Control. d: $p < 0.02$ versus Control. e: $p < 0.02$ versus Control. f: $p < 0.001$ versus Against the attractant. g: $p < 0.001$ versus Control. h: $p < 0.001$ versus Against the attractant.

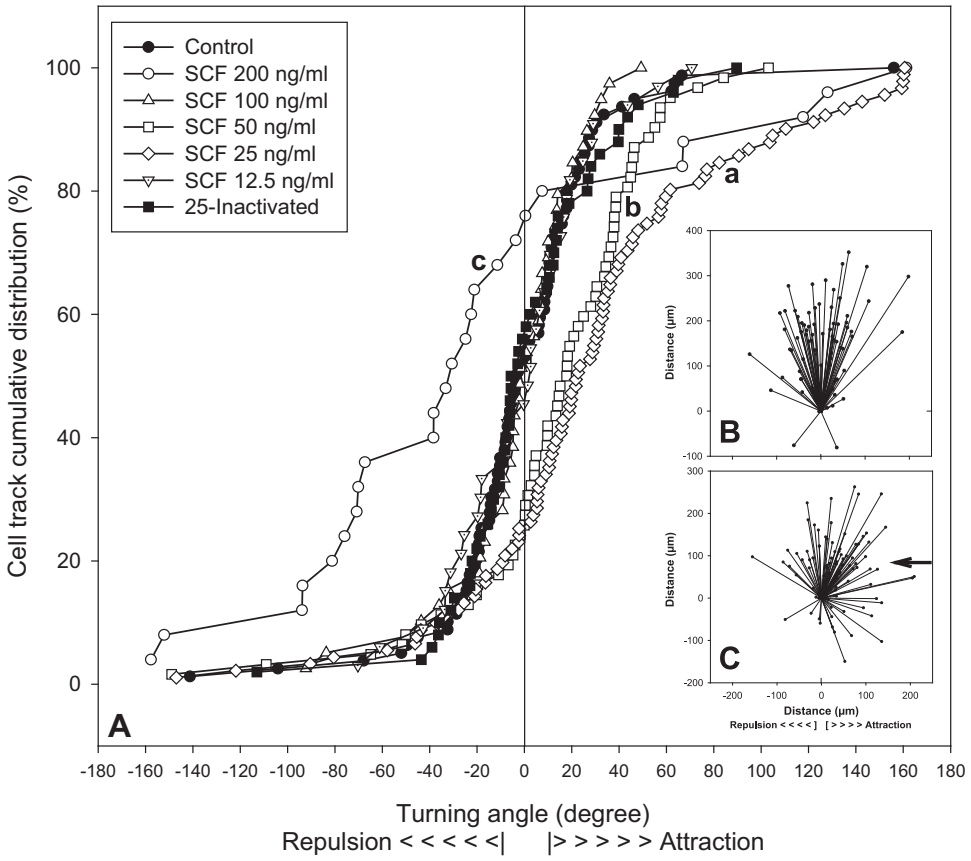

Fig. 11. (A) Distribution of turning angles of NCCs migrating in gradients of different SCF concentrations. Chemotaxis is expressed as cumulative turning angles of cell tracks. For each experimental condition, angular positions of all cells at the end of 6 h of exposure to different SCF concentration gradients are shown in a cumulative distribution plot. The percent value refers to the percentage of cell tracks with angular position less than or equal to a given angular value on abscissa. Significant differences versus control: a: $p < 0.001$; b: $p < 0.003$; c: $p < 0.007$. (B) Linear distance of NCCs migrating in a Zigmond chamber without gradient (control). (C) Linear distance of NCCs migrating in a concentration gradient of 25 ng/ml SCF at the source (arrow).

of the body to differentiate in pigment cells, among many other derivatives (Le Douarin and Kalcheim, 1999).

In the present work, we show that the skin extract (SE) significantly increases NCC number and proliferation, accelerating the appearance of the melanocyte phenotype (Table 1; Figs. 2–4). In addition, following a working hypothesis on the possible influence of epidermal factor(s) on pre-melanocyte colonization (Le Douarin and Kalcheim, 1999), we show that subpopulations of NCCs respond with directional migration along gradients of soluble skin factor(s) (Fig. 5) and of trophic molecule Stem Cell Factor (SCF) (Table 3; Figs. 6–11). These chemotactically-responsive NCCs also showed lengthening shape, increased perimeter and decreased cell area, as well as reduction of speed and greater capacity to maintain rectilinear migration (Table 2), which is consistent with changes observed in directionally migrating cells, and concomitant with typical rearrangements of the actin cytoskeleton (Fig. 7, insets).

The SCF (or steel factor) is a well-known trophic factor, ligand of the receptor tyrosine kinase C-Kit carried by primordial germ cells, hematopoietic stem cells, pre-melanocyte NCCs and NCC-derived neurons (Ashman, 1999; Carnahan et al., 1994; Keshet et al., 1991; Luo et al., 2003). A common factor of these cell lineages is the long distance of oriented migration seen during embryo development, a process that seems strongly related with the SCF/C-Kit system (Yoshida et al., 2001), and with reports that SCF is topologically related with migratory routes of those cell populations (Keshet et al., 1991). From preceding works, it is known that the SCF stimulates in vitro avian NCC survival and melanocyte differentiation (Lahav et al., 1994), and that early avian embryo extracts have proliferative and melanogenic effects on NCCs (Lecoin et al., 1994). Also, in vivo studies showed that during the avian skin development, C-Kit-expressing NCCs migrate into the SDF-producing fields (3–17 days-old avian embryo epidermis) at the time when melanoblasts proliferate and differentiate (Faas and Rovasio, 1998; Lecoin et al., 1995). These and other literature data taken as a whole, together with our present results, indicate that SCF is a qualified diffusible factor of the skin, favoring the proliferation, melanocyte differentiation and directional migration of pre-melanocyte NCCs. Recent reports also show the migration-promoting effect of SCF on other cell types such as cancer cells (Katiyar et al., 2007), neurons of the central nervous system (Erlandsson et al., 2004; Soumiya et al., 2009) and axons (Gore et al., 2008), and also involve this factor in the oriented migration of neural stem cells toward areas of brain injury (Sun et al., 2004).

In the present work, after applying a battery of chemotaxis parameters analyzed under strictly directionality-based criteria, it was noteworthy that the chemotactic behavior of a significant subpopulation of NCCs toward SE and SCF was expressed as the proportion of migrating cells, the distance traveled toward the attractants and the angular bias of the cell trajectories. Moreover, all chemotaxis parameters involving different expressions of oriented cell migration delineated responses with a bell-shaped curve, typical of a concentration-dependent chemotactic response (Blume-Jensen et al., 1993; Erlandsson et al., 2004; Gore et al., 2008). This response to a concentration gradient does not produce a saturation curve of chemotaxis because, when the attractant concentration increases above saturation, specific membrane receptors remain totally occupied, are then incapable of detecting differential changes coming from the extracellular gradient

and, consequently, the chemotactic response falls. The bell-shaped curve was constantly found in the proportion of responding NCCs, the distance traveled and the changes of cell-tracking angle toward the source of the SE/SCF.

Besides the evidence supporting the notion of chemotactic motility of NCCs toward a concentration of 25–50 ng/ml of SCF at the source of the gradient, the NCCs exposed to high concentrations of SCF (100–200 ng/ml) showed an arrested or repulsive migration in relation to the gradient.

The idea of chemorepulsion (or fugetaxis) has been far more studied on leukocytes, contributing greatly in dissecting the molecular mechanisms involved in cell motility toward the tissues and back to vasculature (Huttenlocher and Poznansky, 2008; Mirakaj et al., 2011). Also, the negative guidance of the axon growth cone has received significant attention, from the 1990s classical works (Charron and Tessier-Lavigne, 2005; Song et al., 1998; Tessier-Lavigne and Goodman, 1996) up to recent detailed reports on mechanisms of the in vitro (Rajasekharan et al., 2010) and in vivo (Murray et al., 2010) wiring of the nervous system. On embryonic cells, particularly on NCCs, the evidence of chemorepulsion is scarce, with the exception of some works involving the development of the outflow tract of the heart (Toyofuku et al., 2008), and the early migratory NCCs confined to the trunk ventral pathway (Jia et al., 2005). Recent data show a chemokine system involved in concentration-dependent attraction/repelling phenomena of NCC-derived melanoma cells, associated with tumoral metastatic expansion (Amatschek et al., 2011). A similar concentration-dependent effect of Sonic hedgehog (Shh) was depicted on retinal axons (Kolpak et al., 2009). In addition to the present report, recent evidence from our laboratory also showed the bi-phasic concentration-dependent effect of the chemokine Stromal cell-Derived Factor-1 (SDF-1) (Jaurena, 2011), as well as the morphogen Shh (Tolosa et al., 2011) on the mesencephalic NCCs.

It is important to note that the attraction-repulsion phenomena could be masked by the method of study. Nowadays, a significant proportion of the reports on chemotaxis utilize variants of Boyden's classic across-filter method (Boyden, 1962). As a whole, this static system makes it possible to determine the proportion of cells migrating toward the potential attractant, but not in the opposite sense (Erlandsson et al., 2004). Among the advantages of real-time dynamic study methods, apart from the detection of repulsive cell migration, is the determination of absolute motility parameters such as the cell speed and distance traveled. In this context, the present data show that, at a chemoattractive concentration of SCF (25–50 ng/ml), the NCCs display a significant low cell velocity (see Table 2). This phenomenon was also reported, among others, on neurons of the central nervous system attracted by SCF (Erlandsson et al., 2004) and in our laboratory by the chemokine SDF-1 (Jaurena, 2011) and the morphogen Shh (Tolosa et al., 2011). On the other hand, the chemotactic response of NCCs up to Neurotrophin-3 shows no variation of the cell speed (Zanin and Rovasio, 2010). The mechanism of the cell repulsion phenomena, as well as the relationship between chemotactic orientation and cell velocity, are today still unexplained. In brief, the plausible mechanism to explain chemorepulsion leaves a big question whose answer is still elusive. In fact, there is very little consistent evidence suggesting the general notion that similar molecules drive the cell "forward" or "backward", modulating the opposite directional displacements by very small, but significant, changes in some elements of the complex taxis-associated signal chains (Petersen and Cancela, 2000; Song et al., 1998).

Results from both the present report and previous literature as a whole suggest a simplified general model for in vivo NCC behavior in connection with the SCF/C-Kit system (Fig. 12). The early migratory NCCs, confronted with a spatial low (downward slope) concentration gradient of SCF starting at the epidermis,

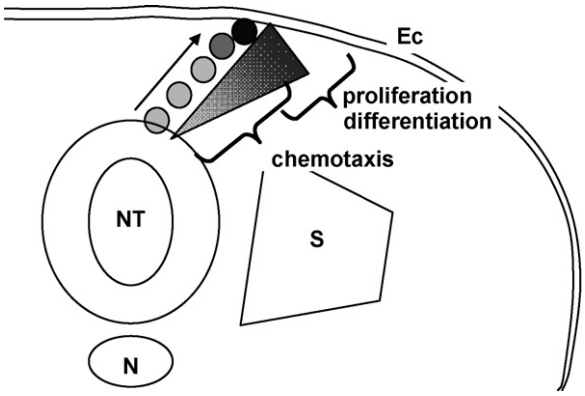

Fig. 12. Schematic transverse section of a vertebrate embryo showing a general chemotactic model of in vivo melanogenic subpopulation of NCCs (spheres). The concentration gradient (shaded triangle) represents epidermal factors (i.e. SCF) that in the downward slope induce chemotactic migration up to gradient (arrow), and at higher concentration stimulate proliferation and melanocytic differentiation of NCCs. Ec: ectoderm (future epidermis = target field). NT: neural tube. S: somite. N: notochord.

respond with an oriented migration toward their destination field (the skin). When arriving in the vicinity of the target gradient source, the higher concentration of chemotactic factor(s) stops the directional guidance but induces a proliferation-survival effect, as well as melanocyte differentiation (Fig. 12). Thus, the continuous growth and expansion of pigment cell lineage could allow their vast skin colonization without necessity of subsequent chemotactic guidance. The assumed factor(s) involved in the SCF gradient formation/stability are not known, whether a source-sink model, SCF consumption by migrating NCCs, or modulation of the SCF shedding in the souce field. The plasticity of the C-Kit receptor, which responds to the concentration-dependent functional signals of the SCF ligand, determining migration, proliferation, survival and/or differentiation of NCCs, is unknown. Many of these phenomena are well known as in vivo morphogenetic changes (Le Douarin and Kalcheim, 1999; Wehrle-Haller et al., 2001). However, we must also consider the probable concomitant influence of other factor(s) such as Fibronectin (Takano et al., 2002), or Endothelin-3 (Dupin et al., 2000; Lahav et al., 1998), which can interact with SCF (Ono et al., 1998), as well as a contribution of the dermis as a possible source of other long-distance molecular cues (Tosney, 2004).

To our knowledge, the present report provides the first direct evidence that SE and SCF modify the directionality of a subpopulation of NCCs, inducing a linearization of cell locomotory behavior, as well as morphologic and dynamic changes typical of oriented migratory cells. The increased persistence of NCCs could participate in the mechanism of skin colonization, by guiding the cells through their surrounding milieu to invade the target field. This observation is consistent with the report of a subpopulation of NCCs recognized by the Mel-EM antibody, an early marker of pigment cells (Lahav et al., 1994). It is generally known that the SCF is expressed in the embryonic epidermis at least from day 3 of development, and the C-Kit receptor is carried by avian pre-melanocyte NCCs (Lecoin et al., 1995) as well as by a sub-population of melanogenic NCCs shortly after their segregation from the neural tube (Luo et al., 2003). Moreover, our present observation, that a large proportion of the leading front NCCs migrating up the gradient of SCF express the C-Kit receptor, suggests that the NCC subpopulation chemotactically responsive to SE and SCF represents the pigment cells subpopulation. The fact that not all, but a significant subpopulation of NCCs respond, is a reflection of the molecular heterogeneity of NCCs. Given that NCCs migrate along different pathways and develop various environment-dependent derivatives (Le Douarin

and Kalcheim, 1999), it is clear that the identity of the complex receptor-cytoplasmic signal chain of NCCs is not homogeneous, and that not all NCCs are necessarily and simultaneously responsive to the SE/SCF stimulus.

Several molecules and mechanisms were proposed as working for the efficient migration of NCCs, from the glycoprotein fibronectin (Rovasio et al., 1983) and other extracellular matrix molecules (Hay, 2005; Lock et al., 2008; Perris and Perissinotto, 2000), to reports suggesting cell-to-cell contacts (Teddy and Kulesa, 2004), the involvement of the Wnt family of genes, the proteoglycan Syndecan-4 and the "planar cell polarity" (Matthews et al., 2008a,b), the mechanism of contact inhibition of locomotion (Carmona-Fontaine et al., 2008) as well as the association between the SCF/C-Kit system and the lateral migration of NCC melanocyte precursors (Wehrle-Haller et al., 2001). These and other studies, using recent technologies on in vivo embryos, provided valuable data for understanding the migration of NCCs (Kulesa et al., 2010; Krispin et al., 2010). However, the persistent motility, contact inhibition phenomena, or even the activity of many extracellular matrix molecules, although important constituents of migratory behavior, may be not exclusively responsible but rather cooperative factor(s) for oriented cell motility. Our in vitro results, obtained with a system that enables the study of NCC subpopulations confronted with concentration gradients of attractants, excluding other migratory factor(s), showed that chemotaxis, studied under strict real-time directional criteria, may be an essential element of spatiotemporal orientation of NCCs toward specific fields of the embryo body, and that NCC-derived pigment cells migrate toward the skin under the SCF/C-Kit system. In addition, in this sensitive process of NCC guidance, it is also reasonable to consider the confluent (also redundant) mechanisms governed by other growth factors and chemokines such as in our not yet published observations (Jaurena, 2011; Tolosa et al., 2011; Zanin and Rovasio, 2010), providing for any failures in the directional behavior of embryonic cells.

In conclusion, our in vitro approach seems to support the idea that diffusible factor(s) of the embryo skin play a crucial role in pigment cell ontogenesis, involving cell proliferation of NCCs, melanocyte differentiation and chemotactically-oriented colonization of the epidermis, induced by a SCF concentration gradient emerging from the skin as the target field (Fig. 12). These data also amplify the functional scope of trophic factors by involving them in new activities as molecular guides for the colonization mechanism of embryonic cells.

Acknowledgements

We thank Mr. Joss Heywood for critical reading of the manuscript. This work was supported by the Consejo Nacional de Investigaciones Científicas y Técnicas (CONICET), the Agencia Nacional de Promoción Científica y Tecnológica (FONCYT), the Ministerio de Ciencia y Tecnología de la Provincia de Córdoba (MINCYT-CBA), and the Secretaría de Ciencia y Tecnología de la Universidad Nacional de Córdoba (SECYT-UNC) (Argentina).

Appendix A. Supplementary data

Supplementary data associated with this article can be found, in the online version, at doi:10.1016/j.ejcb.2011.12.007.

References

Amatschek, S., Lucas, R., Eger, A., Pflueger, M., Hundsberger, H., Knoll, C., Grosse-Kracht, S., Schuett, W., Koszik, F., Maurer, D., Wiesner, C., 2011. CXCL9 induces chemotaxis, chemorepulsion and endothelial barrier disruption through CXCR3-mediated activation of melanoma cells. Br. J. Cancer 104, 469–479.

Ashman, L.K., 1999. The biology of stem cell factor ans its receptor C-Kit. Int. J. Biochem. Cell Biol. 31, 1037–1051.

Belmadani, A., Tran, P.B., Ren, D., Assimacopoulos, S., Grove, E.A., Miller, R.J., 2005. The chemokine stromal cell-derived factor-1 regulates the migration of sensory neuron progenitors. J. Neurosci. 25, 3995–4003.

Blume-Jensen, P., Siegbahn1, A., Stabel, S., Heldin, C.H., Rönnstrand, L., 1993. Increased Kit/SCF receptor induced mitogenicity but abolished cell motility after inhibition of protein kinase C. EMBO J. 12, 4199–4209.

Boldajipour, B., Raz, E., 2007. What is left behind—quality control in germ cell migration. Sci. STKE 383, pe16.

Bottenstein, J.E., Sato, G.H., 1979. Growth of a rat neuroblastoma cell line in serum-free supplemented medium. Proc. Natl. Acad. Sci. U.S.A. 76, 514–517.

Boyden, S.V., 1962. The chemotactic effect of mixtures of antibody and antigen on polymorphonuclear leukocytes. J. Exp. Med. 115, 453–466.

Bradford, M., 1976. A rapid and sensitive method for the quantitation of microgram quantities of protein using the principle of protein-dye binding. Anal. Biochem. 72, 248–254.

Bray, D., 1992. Cell Movements. Garland Publ. Inc., New York.

Carmona-Fontaine, C., Matthews, H.K., Kuriyama, S., Moreno, M., Dunn, G.A., Parsons, M., Stern, C.D., Mayor, R., 2008. Contact inhibition of locomotion in vivo controls neural crest directional migration. Nature 456, 957–961.

Carnahan, J.F., Patel, D.R., Millar, J.A., 1994. Stem cell factor is a neurotrophic factor for neural crest-derived chick sensory neurons. J. Neurosci. 74, 1433–1440.

Charron, F., Tessier-Lavigne, M., 2005. Novel brain wiring functions for classical morphogens: a role as graded positional cues in axon guidance. Development 132, 2251–2262.

Chen, K.C., Ford, R.M., Cummings, P.T., 2003. Cell balance equation for chemotactic bacteria with a biphasic tumbling frequency. J. Math. Biol. 47, 518–546.

Cinamon, G., Grabovsky, V., Winter, E., Franitza, S., Feigelson, S., Shamri, R., Dwir, O., Alon, R., 2001. Novel chemokine functions in lymphocyte migration through vascular endothelium under shear flow. J. Leukoc. Biol. 69, 860–866.

Czirok, A., Zamir, E.A., Szabo, A., Little, C.D., 2008. Multicellular sprouting during vasculogenesis. Curr. Top. Dev. Biol. 81, 269–289.

Dunn, G.A., 1983. Characterising a kinesis response: time averaged measures of cell speed and directional persistence. In: Keller, H., Till, G.O. (Eds.), Leucocyte Locomotion and Chemotaxis. Birkhauser Verlag, Basel, pp. 14–33.

Dupin, E., Glavieux, C., Vaigot, P., Le Douarin, N.M., 2000. Endothelin 3 induces the reversion of melanocytes to glia through a neural crest-derived glial-melanocytic progenitor. Proc. Natl. Acad. Sci. U.S.A. 97, 7882–7887.

Eisenbach, M., 1999. Sperm chemotaxis. Rev. Reprod. 4, 56–66.

Erickson, C.A., 1985. Control of neural crest cell dispersion in the trunk of the avian embryo. Dev. Biol. 111, 138–157.

Erickson, C.A., Goins, T.L., 1995. Avian neural crest cells can migrate in the dorsolateral path only if they are specified as melanocytes. Development 121, 915–924.

Erlandsson, A., Larsson, J., Forsberg-Nilsson, K., 2004. Stem cell factor is a chemoattractant and a survival factor for CNS stem cells. Exp. Cell Res. 301, 201–210.

Faas, L., Rovasio, R.A., 1998. Distribution patterns of neural crest-derived melanocyte precursor cells in the quail embryo. Anat. Rec. 251, 200–206.

Fabro, G., Rovasio, R.A., Civalero, S., Frenkel, A., Caplan, R., Eisenbach, M., Giojalas, L.C., 2002. Chemotaxis of capacitated rabbit spermatozoa to follicular fluid revealed by a novel directionality-based assay. Biol. Reprod. 67, 1565–1571.

Fukuzawa, T., Samaraweera, P., Mangano, F.T., Law, J.H., Bagnara, J.T., 1995. Evidence that MIF plays a role in the development of pigmentation patterns in the frog. Dev. Biol. 167, 148–158.

Gail, M.H., Boone, C.W., 1970. The locomotion of mouse fibroblasts in tissue culture. Biophys. J. 10, 980–993.

Giojalas, L.C., Rovasio, R.A., 1998. Mouse spermatozoa modify their motility parameters and chemotactic response to factors from the oocyte microenvironment. Int. J. Androl. 21, 201–206.

Giojalas, L.C., Iribarren, P., Molina, R., Rovasio, R.A., Estofán, D., 2004a. Determination of human sperm calcium uptake mediated by progesterone may be useful for evaluating unexplained sterility. Fertil. Steril. 82, 738–740.

Giojalas, L.C., Rovasio, R.A., Fabro, G., Gakamsky, A., Eisenbach, M., 2004b. Timing of sperm capacitation appears to be programmed according to egg availability in the female genital tract. Fertil. Steril. 82, 247–249.

Gómez-Moutón, C., Lacalle, R.A., Mira, E., Jiménez-Baranda, S., Barber, D.F., Carrera, A.C., Martínez-A, C., Mañes, S., 2004. Dynamic redistribution of raft domains as an organizing platform for signaling during cell chemotaxis. J. Cell Biol. 164, 759–768.

Gore, B.B., Wong, K.G., Tessier-Lavigne, M., 2008. Stem cell factor functions as an outgrowth-promoting factor to enable axon exit from the midline intermediate target. Neuron 57, 501–510.

Guidobaldi, H.A., Teves, M.E., Uñates, D.R., Anastasía, A., Giojalas, L.C., 2008. Progesterone from the cumulus cells is the sperm chemoattractant secreted by the rabbit oocyte cumulus complex. PLoS ONE 3 (8), e3040, doi:10.1371/journal.pone.0003040.

Hamburger, V., Hamilton, H.L., 1951. A series of normal stages in the development of the chick embryo. J. Morphol. 80, 49–92.

Hay, E.D., 2005. The mesenchymal cell, its role in the embryo, and the remarkable signaling mechanisms that create it. Dev. Dyn. 233, 706–720.

Huttenlocher, A., Poznansky, M.C., 2008. Reverse leukocyte migration can be attractive or repulsive. Trends Cell Biol. 18, 298–306.

Jaurena, M.B., 2011. The chemokine Stromal cell-derived Factor-1 participate in the oriented migration of neural crest cells in normal ontogenesis and exposed to ethanol. PhD Thesis Dissertation, Biology Sciences School, National University of Cordoba, Argentina.

Jaurena, M.B., Carri, N.G., Battiato, N.L., Rovasio, R.A., 2011. Trophic and proliferative perturbations of in vivo/in vitro cephalic neural crest cells after ethanol exposure are prevented by Neurotrophin 3. Neurotoxicol. Teratol. 33, 422–430.

Jia, L., Cheng, L., Raper, J., 2005. Slit/Robo signaling is necessary to confine early neural crest cells to the ventral migratory pathway in the trunk. Dev. Biol. 282, 411–421.

Kasemeier-Kulesa, J.C., McLennan, R., Romine, M.H., Kulesa, P.M., Lefcort, F., 2010. CXCR4 controls ventral migration of sympathetic precursor cells. J. Neurosci. 30, 13078–13088.

Katiyar, S., Jiao, X., Wagner, E., Lisanti, M.P., Pestell, R.G., 2007. Somatic excision demonstrates that c-Jun induces cellular migration and invasion through induction of stem cell factor. Mol. Cell Biol. 27, 1356–1369.

Kee, Y., Hwang, B.J., Sternberg, P.W., Bronner-Fraser, M., 2007. Evolutionary conservation of cell migration genes: from nematode neurons to vertebrate neural crest. Genes Develop. 21, 391–396.

Keshet, E., Lyman, S.D., Williams, D.E., Anderson, D.M., Cosman, D., Jenkins, N.A., Copeland, N.G., Parada, L.F., 1991. Embryonic RNA expression patterns of the C-Kit receptor and its cognate ligand suggest multiple functional roles in mouse development. EMBO J. 10, 2425–2435.

Kolpak, A.L., Jiang, J., Guo, D., Standley, C., Bellve, K., Fogarty, K., Bao, Z.Z., 2009. Negative guidance factor-induced macropinocytosis in the growth cone plays a critical role in repulsive axon turning. J. Neurosci. 29, 10488–10498.

Krispin, S., Nitzan, E., Kassem, Y., Kalcheim, C., 2010. Evidence for a dynamic spatiotemporal fate map and early fate restrictions of premigratory avian neural crest. Development 137, 585–595, doi:10.1242/dev.041509.

Kubota, Y., Ito, K., 2000. Chemotactic migration of mesencephalic neural crest cells in the mouse. Dev. Dyn. 217, 170–179.

Kulesa, P.M., Bailey, C.M., Kasemeier-Kulesa, J.C., McLennan, R., 2010. Cranial neural crest migration: new rules for an old road. Dev. Biol. 344, 543–554.

Kunisada, T., Yoshida, H., Yamazaki, H., Miyamoto, A., Hemmi, H., Nishimura, E., Shultz, L.D., Nishikawa, S.I., Hayashi, S.I., 1998. Transgene expression of steel factor in the basal layer of epidermis promotes survival, proliferation, differentiation and migration of melanocyte precursors. Development 125, 2915–2923.

Lahav, R., Dupin, E., Lecoin, L., Glavieux, C., Champeval, D., Ziller, C., Le Douarin, N.M., 1998. Endothelin 3 selectively promotes survival and proliferation of neural crest-derived glial and melanocytic precursors in vitro. Proc. Natl. Acad. Sci. U.S.A. 95, 14214–14219.

Lahav, R., Lecoin, L., Ziller, C., Nataf, V., Carnahan, J.F., Martin, F.H., Le Douarin, N.M., 1994. Effect of the steel gene product on melanogenesis in avian neural crest cell cultures. Differentiation 58, 133–139.

Lecoin, L., Lahav, R., Martin, F.H., Teillet, M.A., Le Douarin, N.M., 1995. Steel and C-Kit in the development of avian melanocytes: a study of normally pigmented birds and of the hyperpigmented mutant Silky Fowl. Dev. Dyn. 203, 106–118.

Lecoin, L., Mercier, P., Le Douarin, N.M., 1994. Growth of neural crest cells in vitro is enhanced by extracts from Silky fowl embryonic tissues. Pigment Cell Res. 7, 210–216.

Le Douarin, N.M., Brito, J.M., Creuzet, S., 2007. Role of the neural crest in face and brain development. Brain. Res. Rev. 55, 237–247.

Le Douarin, N.M., Dupin, E., 1993. Cell lineage analysis in neural crest ontogeny. J. Neurobiol. 24, 146–161.

Le Douarin, N.M., Kalcheim, C., 1999. The Neural Crest, 2nd edn. Cambridge University Press, Cambridge.

Lohof, M., Quillan, M., Dan, Y., Poo, M.M., 1992. Asymmetric modulation of cytosolic cAMP activity induces growth cone turning. J. Neurosci. 12, 1253–1261.

Lock, J.G., Wehrle-Haller, B., Stromblad, S., 2008. Cell–matrix adhesion complexes: master control machinery of cell migration. Sem. Cancer Biol. 18, 65–76.

Luo, R., Gao, J., Wehrle-Haller, B., Henion, P.D., 2003. Molecular identification of distinct neurogenic and melanogenic neural crest sublineages. Development 130, 321–330.

Marín, C.I., Calamera, J.C., Rovasio, R.A., 1995. Development of an objective, semiautomated method for assessment of sperm motility. Andrologia (Germany) 27, 115–119.

Matthews, H.K., Broders-Bondon, F., Thiery, J.P., Mayor, R., 2008a. Wnt11r is required for cranial neural crest migration. Dev. Dyn. 237, 3404–3409.

Matthews, H.K., Marchant, L., Carmona-Fontaine, C., Kuriyama, S., Larraín, J., Holt, M.R., Parsons, M., Mayor, R., 2008b. Directional migration of neural crest cells in vivo is regulated by Syndecan-4/Rac1 and non-canonical Wnt signaling/RhoA. Development 135, 1771–1780.

McCutcheon, M., Wartman, W.B., Dixon, H.H., 1934. Chemotropism of leukocytes in vitro. Attraction by dried leukocytes, paraffin, glass and staphylococcus albus. Arch. Pathol. 17, 607–614.

Ming, G.L., Song, H.J., Berminger, B., Holt, C.E., Tessier-Lavigne, M., Poo, M., 1997. CAMP-dependent growth cone guidance by Netrin-1. Neuron 19, 1225–1235.

Ming, G.L., Song, H.J., Berminger, B., Inagaki, N., Tessier-Lavigne, M., Poo, M., 1999. Phospholipase C-Y and phosphoinositide 3-kinase mediate cytoplasmic signaling. Neuron 23, 139–148.

Mirakaj, V., Brown, S., Laucher, S., Steinl, C., Klein, G., Köhler, A., Skutella, T., Meisele, C., Brommer, B., Rosenberger, P., Schwab, J.M., 2011. Repulsive guidance molecule-A (RGM-A) inhibits leukocyte migration and mitigates inflammation. Proc. Natl. Acad. Sci. 108, 6555–6560.

Montgomery, D.C., 1991. Design and Analysis of Experiments, 3rd ed. John Wiley & Sons, New York.

Mortimer, D., Fothergill, T., Pujic, Z., Richards, L.J., Goodhill, G.J., 2008. Growth cone chemotaxis. Trends Neurosci. 31, 90–98.

Murray, A., Naeem, A., Barnes, S.H., Drescher, U., Guthrie, S., 2010. Slit and Netrin-1 guide cranial motor axon pathfinding via Rho-kinase, myosin light chain kinase and myosin II. Neural Dev. 5, 16, doi:10.1186/1749-8104-5-16.

Natarajan, D., Marcos-Gutierrez, C., Pachnis, V., de Graaff, E., 2002. Requirement of signalling by receptor tyrosine kinase RET for the directed migration of enteric nervous system progenitor cells during mammalian embryogenesis. Development 129, 5151–5160.

Ng, K.L., Li, J.D., Cheng, M.Y., Leslie, F.M., Lee, A.G., Zhou, Q.Y., 2005. Dependence of olfactory bulb neurogenesis on prokineticin 2 signaling. Science 308, 1923–1927.

Noble, P.B., Levin, M.D., 1986. Computer-assisted Analyses of cell Locomotion and Chemotaxis. CRC Press, Inc., Boca Raton, FL, USA.

Oliveira, R.G., Tomasi, L., Rovasio, R.A., Giojalas, L.C., 1999. Increased velocity and induction of chemotactic response in mouse spermatozoa by follicular and oviductal fluids. J. Reprod. Fertil. 115, 23–27.

Ono, H., Kawa, Y., Asano, M., Ito, M., Takano, A., Kubota, Y., Matsumoto, J., Mizoguchi, M., 1998. Development of melanocyte progenitors in murine Steel mutant neural crest explants cultured with stem cell factor, endothelin-3, or TPA. Pigment Cell Res. 11, 291–298.

Paratcha, G., Ibañez, C.F., Ledda, F., 2006. GDNF is a chemoattractant factor for neuronal precursor cells in the rostral migratory stream. Mol. Cell Neurosci. 31, 505–514.

Perris, R., 1987. Cell-matrix interactions in neural crest development. PhD Thesis. Uppsala University. Sweden.

Perris, R., Perissinotto, D., 2000. Role of the extracellular matrix during neural crest cell migration. Mech. Dev. 95, 3–21.

Petersen, O.H., Cancela, J.M., 2000. Attraction or repulsion by local Ca^{2+} signals. Curr. Biol. 10, R311–R314.

Provance, D.W., Wei, M., Ipe, V., Mercer, J.A., 1996. Cultured melanocytes from dilute mutant mice exhibit dendritic morphology and altered melanosome distribution. Proc. Natl. Acad. Sci. U.S.A. 93, 14554–14558.

Rajasekharan, S., Bin, J.M., Antel, J.P., Kennedy, T.E., 2010. A central role for RhoA during oligocendroglial maturation in the switch from Netrin-1-mediated chemorepulsion to process elaboration. J. Neurochem. 113, 1589–1597.

Ramón y Cajal, S., 1892. La rétine des vertebrés. La Cellule 9, 119–258.

Richardson, M.K., Sieber-Blum, M., 1993. Pluripotent neural crest cells in the developing skin of the quail embryo. Dev. Biol. 157, 348–358.

Rovasio, R.A., Delouvée, A., Yamada, K.M., Timpl, J.P., Thiery, J.P., 1983. Neural crest cell migration: requirements for exogenous fibronectin and high cell density. J. Cell Biol. 96, 462–473.

Rovasio, R.A., Battiato, N.L., 1996. Changes of morphological parameters of in vitro migrating neural crest cells induced by ethanol. Comun. Biol. 14, 141–149.

Rovasio, R.A., Battiato, N.L., 2002. Ethanol induces morphological and dynamic changes on in vivo and in vitro neural crest cells. Alcohol: Clin. Exper. Res. 26, 1286–1298.

Rovasio, R.A., Giojalas, L.C., Marín, C.I., 1994. Three seconds is an efficient tracking time to distinguish different mouse sperm motility patterns. Comun. Biol. 12, 313–320.

Sauka-Spengler, T., Bronner-Fraser, M., 2008. A gene regulatory network orchestrates neural crest formation. Nat. Rev. Mol. Cell Biol. 9, 557–568.

Song, H.J., Ming, G.L., He, Z., Lehmann, M., McKerracher, L., Tessier-Lavigne, M., Poo, M.M., 1998. Conversion of neural growth cone responses from repulsion to attraction by cyclic nucleotides. Science 281, 1515–1518.

Song, H.J., Ming, G.L., Poo, M.M., 1997. cAMP-induced switching in turning direction of nerve growth cone. Nature 388, 275–279.

Soumiya, H., Fukumitsu, H., Furukawa, S., 2009. Stem cell factor induces heterotopic accumulation of cells (heterotopia) in the Mouse cerebral cortex. Biomed. Res. 30, 121–128.

Sun, F., Giojalas, L.C., Rovasio, R.A., Tur-Kaspa, I., Sanchez, R., Eisenbach, M., 2003. Lack of species-specificity in mammalian sperm chemotaxis. Dev. Biol. 255, 423–427.

Sun, L., Lee, J., Fine, H.A., 2004. Neuronally expressed stem cell factor induces neural stem cell migration to areas of brain injury. J. Clin. Invest. 113, 1364–1374.

Takano, N., Kawakami, T., Kawa, Y., Aasano, M., Watabe, H., Ito, M., Soma, Y., Kubota, Y., Mizoguchi, M., 2002. Fibronectin combined with stem cell factor plays an important role in melanocyte proliferation, differentiation and migration in cultured mouse neural crest cells. Pigment Cell Res. 15, 192–200.

Teddy, J.M., Kulesa, P.M., 2004. In vivo evidence for short- and long-range cell communication in cranial neural crest cells. Development 131, 6141–6151.

Teillet, M.A., 1971. Recherche sur la mode de migration et la differentiation des melanoblastes cutanes chez l'embryon d'oiseau. Ann. Embryol. Morphol. 4, 95–109.

Tessier-Lavigne, M., Goodman, C.S., 1996. The molecular biology of axon guidance. Science 274, 1123–1133.

Teves, M.E., Barbano, F., Guidobaldi, H.A., Sanchez, R., Miska, W., Giojalas, L.C., 2006. Progesterone at the picomolar range is a chemoattractant for mammalian spermatozoa. Fertil. Steril. 86, 747–749.

Thibodeau, G., Frost-Mason, S.K., 1992. Inhibition of neural crest cell differentiation by embryo ectodermal extract. J. Exp. Zool. 261, 431–440.

Tolosa, E.J., Battiato, N.L., Rovasio, R.A., 2011. Involvement of Sonic hedgehog protein on mesencephalic neural crest cells migration. In: 3rd Meeting of Young Neuroscientists, Córdoba, Argentina.

Tosney, K.W., 2004. Long-distance cue from emerging dermis stimulates neural crest melanoblast migration. Dev. Dyn. 229, 99–108.

Toyofuku, T., Yoshida, J., Sugimoto, T., Yamamoto, M., Makino, N., Takamatsu, H., Takegahara, N., Suto, F., Hori, M., Fujisawa, H., Kumanogoh, A., Kikutani, H.,

2008. Repulsive and attractive semaphorins cooperate to direct the navigation of cardiac neural crest cells. Dev. Biol. 321, 251–262.
van Haastert, P.J., Keizer-Gunnink, I., Kortholt, A., 2007. Essential role of PI3-kinase and phospholipase A2 in Dictyostelium discoideum chemotaxis. J. Cell Biol. 177, 809–816.
von Philipsborn, A., Bastmeyer, M., 2007. Mechanisms of gradient detection: a comparison of axon pathfinding with eukaryotic cell migration. Int. Rev. Cytol. 263, 1–62.
Wang, Y., Ding, S.J., Wang, W., Jacobs, J.M., Qian, W.J., Moore, R.J., Yang, F., Camp 2nd, D.G., Smith, R.D., Klemke, R.L., 2007. Profiling signaling polarity in chemotactic cells. Proc. Natl. Acad. Sci. U.S.A. 104, 8328–8333.
Wehrle-Haller, B., Meller, M., Weston, J.A., 2001. Analysis of melanocyte precursors in Nf1 mutants reveals that MGF/KIT signaling promotes directed cell migration independent of its function in cell survival. Dev. Biol. 232, 471–483.
Yoshida, H., Kunisada, T., Grima, T., Nishimura, E.K., Nishioka, E., Nishikawa, S.I., 2001. Melanocyte migration and survival controlled by SCF/C-Kit expression. J. Invest. Derm. Symp. Proc. 6, 1–5.
Young, H.M., Bergner, A.J., Anderson, R.B., Enomoto, H., Milbrandt, J., Newgreen, D.F., Whitington, P.M., 2004. Dynamics of neural crest-derived cell migration in the embryonic mouse gut. Dev. Biol. 270, 455–473.
Zacchei, A.M., 1961. Lo sviluppo embrionale della quaglia giapponese (Coturnix coturnix japonica T. e S.). Arch. Anat. 60, 36–62.
Zanin, J.P., Rovasio, R.A., 2010. Guiding role of Neurotrophin-3 on directional migration of neural crest cells. In: 25th Meeting of the National Society for Neurosciences Research, Cordoba, Argentina.
Zheng, J.Q., Felder, M., Connor, J.A., Poo, M.M., 1994. Turning of nerve growth cones induced by neurotransmitters. Nature 368, 140–144.
Zigmond, S.H., 1977. Ability of polymorphonuclear leukocytes to orient in gradient of chemotactic factors. J. Cell Biol. 75, 606–616.